POLITECNICO DI TORINO
Repository ISTITUZIONALE

Modelling and validation of a single-storey flexible double-skin façade system with a building energy simulation tool

(Article begins on next page)

20 March 2024

Modelling and validation of a single-storey flexible double-skin façade system with a building energy simulation tool

Elena Catto Lucchino [a], Giovanni Gennaro [b,c], Fabio Favoino [b], Francesco Goia [a,*]

[a] Department of Architecture and Technology, Norwegian University of Science and Technology, NTNU, Trondheim, Norway
[b] Department of Energy, Politecnico di Torino, Torino, Italy
[c] Institute for Renewable Energy, EURAC Research, Bolzano, Italy

A B S T R A C T

Double skin façades are adaptive envelopes designed to improve building energy use and comfort performance. Their adaptive principle relies on the dynamic management of the cavity's ventilation flow and, when available, of the shading device. They can also be integrated with the environmental systems for heating, cooling, and ventilation. However, in most cases, the possible exploitation of the ventilation airflow is not fully enabled, as the adoption of only one or two possible airpath limits the possibility that this façade architecture offers, meaning that flexible interaction with the environmental systems cannot be planned. This work aims to develop, using an existing software tool for building energy simulation, a numerical model of a flexible double-skin façade module capable of fully exploiting the adaptive features of such an envelope concept by switching between different cavity ventilation strategies. Leveraging the "Double Glass Facade" component available in IDA ICE, a new model for a flexible double-skin façade module was developed, and its performance in replicating the thermophysical behaviours of such a dynamic system was assessed by comparison with experimental data collected through a dedicated experimental activity using one the outdoor test cells of the TWINS facility in Torino (Italy). The accuracy of the predictions of the new model for a flexible double-skin façade was in line with that obtained by the conventional "Double Glass Facade" component to simulate traditional double-skin facades. The mean bias errors obtained were lower than 1.5 °C and 4 W/m^2, for air and surface temperature values and for transmitted long-wave or short-wave heat flux values, respectively. By establishing a new archetype model to study the performance and optimal integration of a large class of double-skin façade modules, including fully flexible ones, this work demonstrates the possibility of modifying existing models in building energy simulation tools to study unconventional building envelope model solutions such as adaptive façade systems.

1. Introduction

1.1. Background and research relevance

Double skin façades (DSFs) are highly transparent envelope technologies that can dynamically adjust their thermo-optical properties in response to transient boundary conditions (either external, such as climate, or internal, such as occupants' requirements). Such adaptive behaviour can allow the exploitation of solar energy for both passive solar thermal gains and daylighting, which can reduce energy use for building climatisation [1] and provide better thermal and visual comfort conditions compared to a traditional single-skin façade [2]. An important adaptive principle in a DSF is the dynamic management of the

ventilation flow in the façade cavity [3], often in combination with a shading system installed in the cavity to achieve variable performance goals. In most cases, however, the possible exploitation of the ventilation airflow is limited to just one or two options: only *outdoor air curtain* (OAC) ([4–9]); only *supply air* (SA) [10]; OAC and e*xhaust air* (EA) [11]; i*ndoor air curtain* IAC and OAC [12]; *thermal buffer* TB and OAC [13,14]; or TB and SA [15]. This conventional approach significantly reduces the possibility of fully exploiting the conceptual flexibility offered by this façade architecture as, in theory, both the inlet side (either outdoor air or indoor air) and the outlet side (again, towards the inside or the outside) can be combined to obtain a significant variation in the performance of the façade.

Moreover, the dynamic integration between a ventilated façade and the HVAC system could also play a significant role in enhancing the

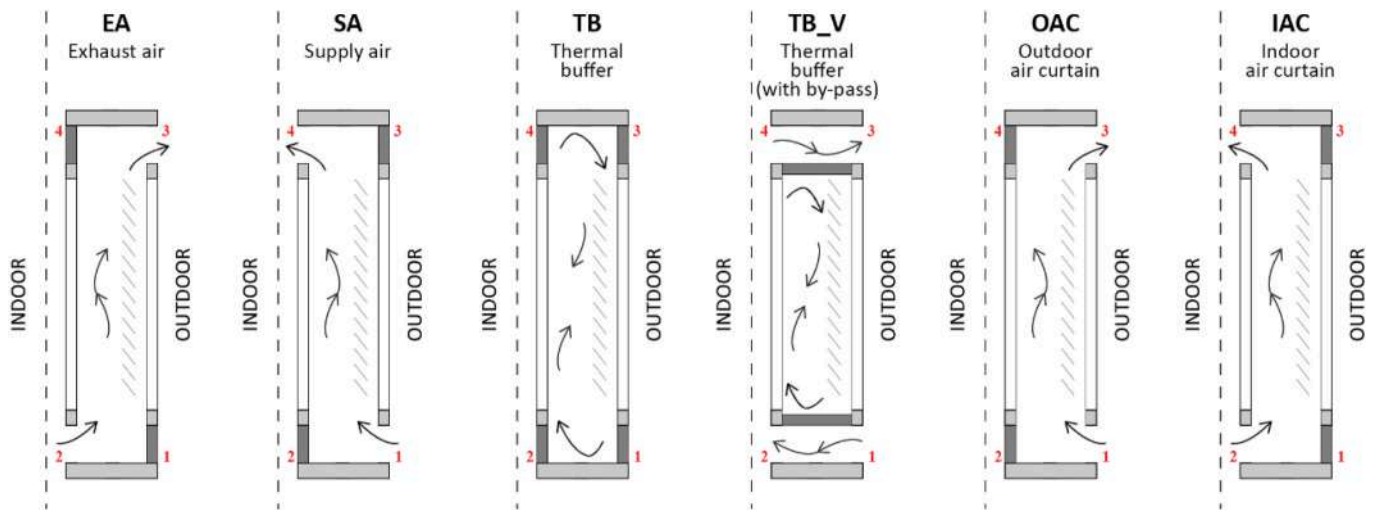| Acronym list		Nomenclature	
		g	solar factor $(-)$
BES	building energy simulation	λ	thermal conductivity of air (W/mK)
CV(RMSE)	coefficient of variation of the root mean square error	M_i	Measured value at one point
DSF	double skin facade	n	Total number of measurements
EA	exhaust air	P_i	Simulated predicted value
IAC	indoor air curtain	ρ_{in}	glazing solar reflectance, inner face $(-)$
OAC	indoor air curtain	ρ_{out}	glazing solar reflectance, outer face $(-)$
SA	supply air	s	thickness (mm)
TB	thermal buffer	τ_{sol}	glazing solar transmittance $(-)$
MBE	mean bias error	U	glass thermal transmittance (W/(m^{2}K))
NMBE	normalised mean bias error	U_f	frame thermal transmittance (W/(m^{2}K))
RMSE	root mean squared error		

Fig. 1. Ventilation strategies implementable in a fully flexible DSF module.

adaptive behaviour of a façade, yet this feature has been rarely investigated so far [16]. Doing so could open new possibilities to further improve the overall performance of the building, e.g., by reducing the demand for mechanical ventilation if the conditions for supplying fresh air through the façade are met. By stretching the borders of the existing concept of DSFs, playing with the airflow path, the airflow type (mechanically or naturally driven), the interplay with the solar shading system, and the overall integration with the HVAC elements in the buildings, one could thus, in theory, enable a vast range of variability in the façade.

The advantages and performance linked to the dynamic exploitation of different airflow paths and a variable integration with the HVAC system have been rarely explored in real cases and also at the research level. Park and co-authors [17,18] developed a lumped model of a flexible DSF with calibration with in-situ measurements and tested it with an optimised control strategy; the developed model allowed for ten different natural ventilation strategies, together with varying positions of shading and opening degrees. Later studies by the same authors adopted a co-simulation approach between an improved version of the previously developed lumped model [19] and a building energy simulation (BES) tool [20], achieving better results than using a zonal method.

As demonstrated by the previous studies, a detailed simulation of the thermal, fluid mechanic, and optical behaviour of a DSF is necessary to test and optimise the behaviour of such a façade concept. The coupling between such an envelope model and a whole building energy simulation (BES) tool is essential for correctly assessing the interplay between the envelope system and the overall building environmental systems and, consequently, the overall performance of this concept. Only a few BES tools include dedicated modules for DSFs' simulation [21], but none allow the façade to adopt different ventilation strategies within the same simulation run, which is one of the gaps in existing models of DSF systems for BES tools [22]. Currently, the simulation of a flexible DSF system with a BES tool can only be carried out by co-simulation, a process that presents advantages and a series of limitations and challenges - such as the need to develop a dedicated model for the flexible DSF and to couple it with a BES tool.

The scope of the research presented in this paper covers the possibilities and challenges of simulating a flexible double-skin façade system using existing software tools for building energy simulation without the need to resort to co-simulation. The research showcases how existing structures in established software environments can be modified to meet the modelling requirements for building envelope systems that go beyond the current possibilities in the specific tool. The elements of innovation of this research can be summarised in the list below:

- a new DSF model archetype, based on the calculation routines for DSFs available in the tool IDA ICE, where ventilation air path and driving force can be continuously changed during the simulation runtime, as well as the interaction between the façade and the HVAC of the building;
- a comprehensive validation of the DSF model archetype using experimental data, covering different airflow paths, and driving forces, which demonstrates the reliability of the numerical model,
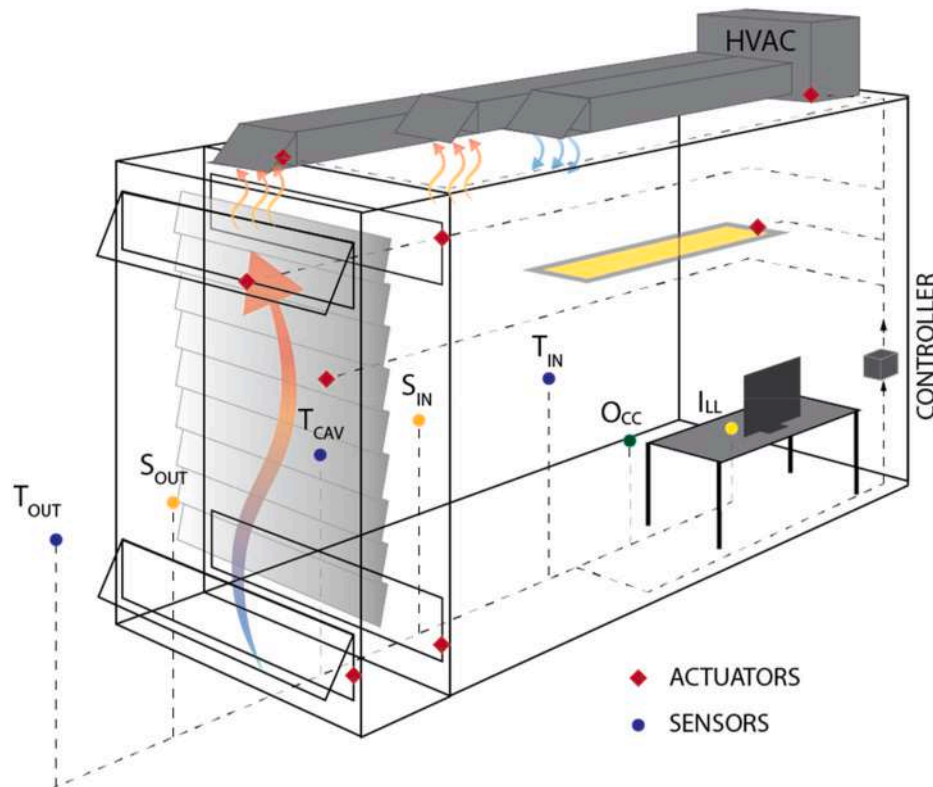
Fig. 2. Integration between the room systems and a DSF.

using data collected through a dedicated experimental activity where a façade prototype was installed on one outdoor test cell of the TWINS facility in Torino (Italy)

- the flexible DSF system model is made publicly available through a repository [23].

1.2. Research aims and objectives, manuscript structure and target audience

The primary aim of the research activity was to develop and validate a numerical model of a flexible double-skin façade system with a building energy simulation (BES) tool. Beyond showcasing how BES tools can be modified to simulate more advanced façade systems, the need for a flexible DSF module arose from a dedicated research project on this façade concept. As explained in more detail in the following sections, the core of the dynamic facade concept explored in this research is a flexible DSF module capable of switching between different cavity ventilation strategies (Fig. 1): exhaust air (EA), supply air (SA), outdoor air curtain (OAC), indoor air curtain (IAC) and thermal buffer (TB), and ventilated thermal buffer (TB_V)), coupled with different airflow-inducing mechanisms (i.e., either a natural (N) or a mechanical (M) airflow (a feature that increases the complexity of the operations of the façade element drastically), and therefore interplay with the HVAC plant of the building.

The secondary aim of this activity was to provide the building simulation community and the design community with a single-storey DSF model archetype that could be used not only in its most extreme configuration (with full flexibility in the ventilation airflow path) but also as a standard model to explore better operations for more conventional single-storey DSF modules. Such a model overcomes the current limitations of conventional DSF models in BES tools. Furthermore, given the validation procedure carried out in this study, the reliability of this flexible numerical model has been checked over a large range of operational modes.

The choice of the BES tool employed in this activity builds on a previous study [21], which showed that only a few tools embed routines for modelling a DSF: IDA ICE, EnergyPlus, and TRNSYS. In the latter two tools, these in-built components only model mechanically ventilated facades. Conversely, IDA ICE's component allows the modelling of DSFs with both natural and mechanical cavity ventilation through the in-built component called *"Double Glass Facade"*. This in-built module, presented in the next section, is already integrated into the thermal and airflow network of the BES tool and allows the combined simulation between the façade component and the indoor space.

IDA ICE (IDA Indoor Climate and Energy) is a BES software that supports the simulation of multi-zonal indoor climate phenomena and energy use in buildings when subjected to transient state boundary conditions. It implements state-of-the-art models, and it has been validated according to the relevant international standards (e.g., ISO 13791, now ISO 52016–1:2017 [24]; EN 15255 and 15,265 [25], ASHRAE 140 [26]). IDA ICE is a differential-algebraic equation (DAE) based tool with a library written in neutral model format (NMF) [27,28]. This allows editing the components' connections in a relatively free way (at least compared to the other tools), leading to the possibility of implementing a more flexible model without resorting to establishing co-simulation routines – a frequently necessity in many BES tools when modelling advanced building envelope concepts which structures are not available in numerical representations embedded in these tools, or when multiple physical (and performance) domains need to be simultaneously represented, sometimes with different levels of model complexity [29]. The already available openness of the DSF routine in IDA ICE, together with the overall performance in replicating the thermophysical and optical behaviour of DSF, was the reason for selecting this tool for this research. The *"Double Glass Facade"* option is used in a basic simulation model, and it is then further developed and modified to meet the functionality requirement identified for the flexible DSF module concept.

The overall research design was broken down into a series of steps that are described by the following objectives: i) to identify a suitable

BES tool and, by leveraging its functionalities, to define a numerical representation of the flexible DSF concept (model development); ii) to collect a series of experimental data on a physical mock-up of a flexible DSF system under outdoor boundary conditions and dynamic control sequences; iii) to replicatethe experiments using measured boundary conditions in BES environment; iv) to analyse and compare (both qualitatively and quantitatively) the simulation output of some selected physical quantities at façade level with the correspondent experimental values (model validation) in order to verify the reliability of the newly developed flexible DSF model.

To present the different objectives of the research design, the article is organised as follows. In *Section 2 – DSF-based adaptive façade concept and numerical model in a BES tool,* we provide the reader with a brief overview of the current possibilities and performance of DSF's simulation with different BES tools, and we present the first objective of the research activity, i.e., we describe how the enhanced model that allows the façade to be operated with different airflow paths/regimes was developed in the selected BES tool (IDA ICE). *In Section 3 – Experimental set-up and data collection for model validation–* we present information about a case-study façade prototype used to collect experimental data. In *Section 4 – Numerical model validation: methods, results, and discussion,* we describe how the experiments were replicated in a simulation environment by using the flexible DSF model, and we show the comparison between experimental data and numerical data to assess the reliability of the newly developed model. The conclusive summary of the paper is presented in *Section 5 – Conclusions.*

The research presented in this paper targets both the R&D community and the professional community. The concept of the highly flexible adaptive facade and its numerical model can be relevant for the first group, which can further investigate the performance of this concept and expand the knowledge about the challenges and possibilities in modelling (and controlling) advanced façade systems in BES. Furthermore, the experimental dataset used in this process is also openly shared in a repository for any researcher to use for model validation or performance analysis purposes. In this article, the professional community can find a demonstration of how to exploit existing BES tools to model advanced functionalities for building envelope systems that are not found in the modules embedded in the release of a BES. The flexible DSF model is also made available to stimulate the design and assessment of more advanced DSF systems that can exploit a broader range of operational modes.

2. DSF-based adaptive façade concept and its numerical model in a BES tool

2.1. Enabling adaptive behaviour through a flexible double-skin façade concept

The motivation that drives this study's development is to evolve the double skin façade/window architecture and to combine it with an integrated embedded control system in interaction with different elements of the building HVAC system to realise a flexible envelope component. This adaptive façade concept exploits different cavity ventilation paths with both mechanically and naturally driven airflows, allows the by-pass of the ventilated cavity if desired, and manages the direct solar and luminous gain through an integrated shading system (Fig. 2) in coordination with the building energy management system. One of the core elements of this façade system is the inlet and outlet section, which contains an actuator that makes it possible to easily switch between different ventilation paths. For reasons linked to IPR (Intellectual Property Rights), full details of this component cannot be provided here. Another core aspect of this façade system is that it integrates an embedded controller that manages the different actuators in the façade module (not only the inlet/outlet sections but also the integrated shading device and fans) and interacts with a supervisory level controller to ensure that the optimal control of the façade-level is jointly managed with the other types of equipment in the building.

This façade module is thus a dynamic element that, under the coordination of the room-level controller, becomes a part of an integrated envelope-HVAC system and actively contributes to balancing energy and indoor environmental quality requirements. In fact, to truly exploit the potential of such a fully flexible DSF vision, total variability across different aspects and components is the key to exploiting this highly dynamic element. As such, the performance of this adaptive building envelope system depends not only on the possibility of adapting its performance through changing its functioning modes but also on how such shift between the multiple operational modes is continuously controlled during operation (i.e., the control strategy) [30].

2.2. Modelling requirements, possible approaches and available in-built modules

A reliable numerical representation of the above-described adaptive façade concept based on a flexible DSF system is necessary to analyse the performance of the innovation idea, optimise its design, and define suitable control strategies for its operation. Detailed simulation of the thermal, fluid mechanics and optical behaviour of double skin facades/windows can be obtained using different approaches, such as custom-built models [17,18,31] or dedicated CFD (Computational Fluid Dynamics) simulations [32,33]. However, in terms of modelling requirements, a very dynamic envelope system must allow easy connectivity with other models that reproduce the heat and luminous balance of a closed space, as well as representations of other HVAC components that may become integrated players in the integration of a dynamic façade concept into a room. The coupled simulation of the whole building and the specific building components is essential to correctly assess the overall energy and comfort performance and replicate the complex interaction between airflow in the façade, the HVAC system, and the building energy management system. Finally, it is also the best way to study how a local strategy to control the façade is integrated into the overall building control strategy to ensure that both the envelope and environmental system for building climatisation act towards the same goal.

In this context, Building Energy Simulation (BES) tools are a good trade-off simulation environment to enable the complete study of adaptive envelope systems in connection with the rest of the building, even considering their limitations. BES tools have generally been developed to simulate the variation of physical conditions in the indoor space and calculate the necessary energy use to maintain the indoor space within a given range of conditions. Since they derive from the need to simulate the overall building performance, BES environments have not been designed to easily model and simulate adaptive facades, as the envelope is just a component of a broader system [34]. However, some possibilities exist to model adaptive façade systems by modifying the existing embedded modules suitably without exploring more advanced strategies such as co-simulation [29]. For example, the implementation of DSFs in BES is possible and has been widely explored in the past. A few BES tools include dedicated modules for DSFs' simulation [35]. However, no BES tool natively consists of the features that would allow one to model the highly flexible facade concept put forward in this research, as the few modules available present limitations regarding fully flexible cavity ventilation paths, alternation of ventilation mechanisms, different integration with the HVAC, etc. [21].

Different approaches are available to model the DSF, either through in-built modules or the so-called zonal approach [36]. The zonal approach divides the cavity into several thermal zones stacked vertically. The zones are connected through an airflow network representation that allows one to describe the airflow through the different zones. The effeect of the number of stacked thermal zones on the quality and reliability of the simulation has been previously explored [7,12], but there is no consensus nor a standardised approach when it comes to this setting, which usually ranges (when referred to as single-storey DSFs)
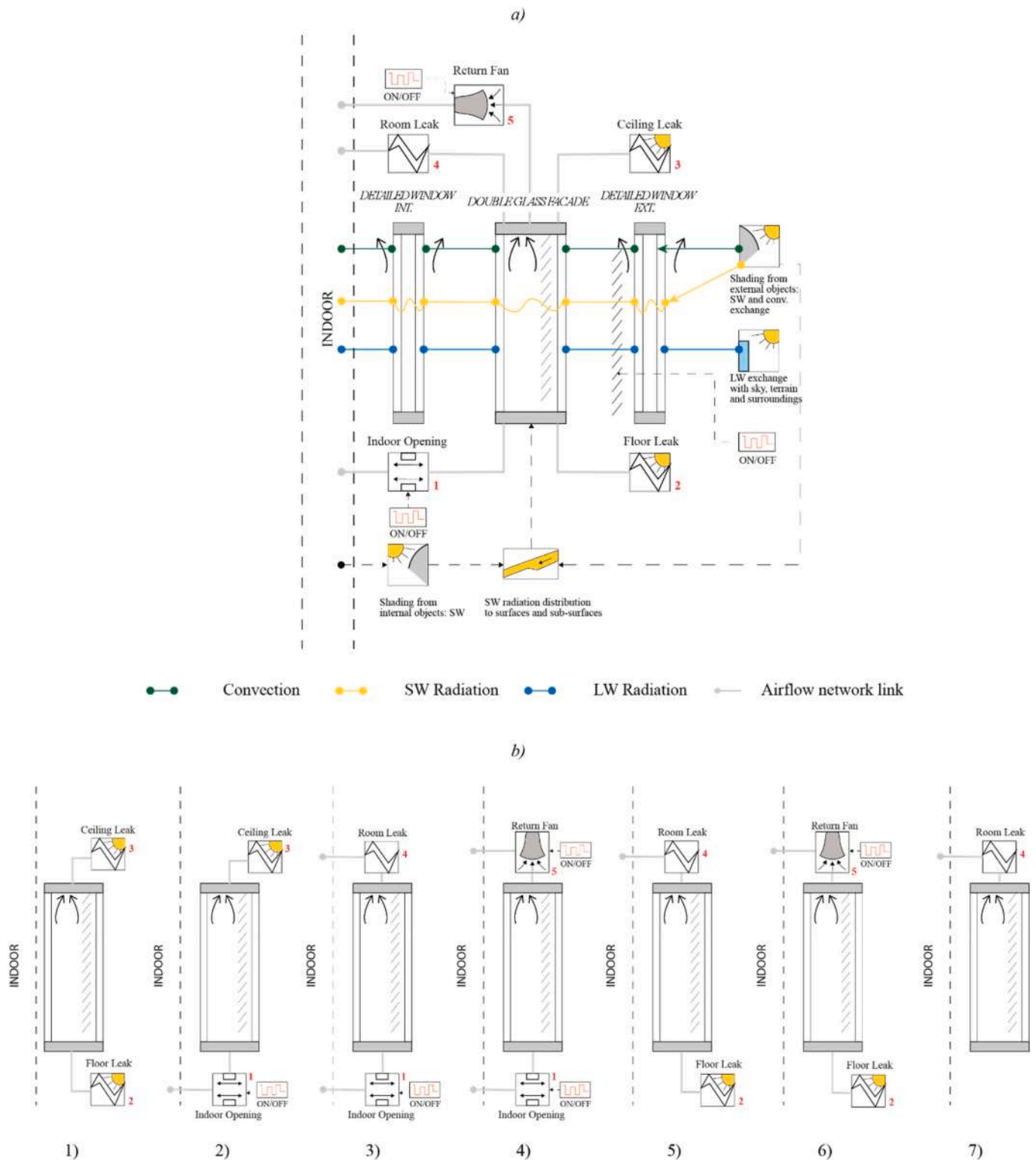
Fig. 3. a) Schematic view of the 'Double Glass Façade' component as implemented in IDA ICE with the different air links available (only one ventilation strategy at a time is implementable in a model) – b) Ventilation strategies that can be modelled using the component: 1) OAC_N, 2) OAC_M, 3) IAC_N, 4) IAC_M, 5) SA_N, 6) SA_M, and 7) TB.

from a minimum of one to a maximum of six.

The other modelling possibility available in some tools is to use an in-built module; a sub-routine dedicated to modelling DSF systems. These sub-models belong to the building envelope systems category and are objects linked to the other components of the simulated environment according to the requirements and possibilities set by each tool. While,

on the one hand, this approach should lead to more accurate simulation (as the models for DSF are purposefully developed to replicate the thermal-fluid behaviour of these systems), on the other hand, this approach is usually less flexible than the approach where the modeller creates an ad-hoc, combined thermal and airflow network.

In a previous analysis covering several tools [21], we identified

different modelling approaches and possibilities to simulate DSFs in BES environments. A few simulation environments (EnergyPlus, IDA ICE and TRNSYS) offer dedicated in-built modules to simulate DSFs. In particular, IDA ICE's module for DSF simulation, called *"Double Glass Facade"*, allows the modelling of both naturally driven and mechanically driven DSFs and their dynamic interaction with the indoor space and the environmental systems. This model is suitable for transient state simulations and even includes the effect of the glazed layers' thermal inertia features–a feature not available in any of the other in-built modules embedded in different BES tools.

Another significant feature addressed by IDA ICE is the relatively easy definition of ad-hoc-developed decision trees that can control both façade and HVAC components. From the perspective of a flexible DSF system that can change the flow path and interact with the environmental systems (e.g., supply fresh air for ventilation in place of the mechanical ventilation plant, or act as an exhaust terminal for the ventilation plant), the smooth shift between the multiple, HVAC-integrated operational modes via combined control strategies is an important asset.

However, the in-built module does not present the level of flexibility necessary to meet the goals set for this research activity and will be modified, as explained more in detail in section 2.3.2, to satisfy the performance requirements set for the simulation model of a fully flexible DSF system.

2.3. Model implementation in IDA-ICE environment

In general, IDA ICE allows modelling with three different user interface levels [28]. At the most superficial level, called *Wizard*, the scope is limited to a specific type of study and level of approximation. The user can perform a simulation directly or transfer the data entered to the next level, called the *Standard* level. The user is given greater freedom to design a building model at the standard level. At this level, geometry, materials, controller settings, loads, etc., are defined, and some of them (geometry, external shadings, etc.) are not modifiable further at the next level, called the *Advanced* level. Here the simulation model is no longer defined in physical terms, but as connected component models defined by equations. All equations, parameters and variables can be examined, and the time evolution of variables can be studied.

Moreover, new connections between components can be created using the advanced modelling level, and a more comprehensive range of modelling strategies can be adopted. Furthermore, more advanced control strategies can be implemented, too, i.e., the controllable components can be connected to a schedule, or a control logic defined within the software with a relatively flexible and user-friendly interface. The advanced level was therefore employed in this work. In the first of the following sub-sections, we will describe how a DSF can be modelled at the standard level and which limitations this model presents (2.3.1); in the second sub-section (2.3.2), the modifications necessary to model a fully flexible DSF are presented.

2.3.1. Double Glass Facade component

DSFs can be modelled in IDA ICE at the standard level, using a 'Detail Window Model' component and enabling the possibility of adding a ventilated cavity: a window (which models the DSF as a box window) or wall (which models it as a ventilated wall of the same height as the external wall).

The ventilated cavity component is called *"Double Glass Façade"*- Fig. 3-a), and in it, the averaged cavity-air temperature is calculated based on the inlet temperature, mass flow and solar gains and heat transferred through the surfaces. The component calculates only one temperature for the whole façade, so the effects of the air stratification are not represented in an explicit way. The model geometry is two-dimensional; consequently, heat transferred through the sidewalls of the cavity is excluded from the energy balance calculation.

The *"Detail Window Model"*, both for the interior and exterior skin, adopts a layer-by-layer computation of multiple reflections, and each layer's temperature is computed according to ISO 15099 [37]. The shading layer, if present, needs to be modelled as part of one of the two detailed windows – as such, its properties are calculated according to the ISO 15099 (in case of spectral data being provided, both for the shading device and the glass layers, the calculation method adopted is the one of the ISO 52022–3 [38]). It is recommended to model it as an internal shade of the outer pane [39]. Two different calculation methods (e.g., convection coefficients, airflow, etc.) are adopted on each side of the shading device. One side is modelled as part of the *"Detail Window Model"* element, and the other is part of the *"Double Glass Façade"*. This is the one used in the air mass balance calculation.

From the standard level, as summarised in Fig. 3 a, the *"Double Glass Façade"* component allows five possible air-links to the cavity: *1* - an operable opening towards the zone; *2* - a leakage area at the floor and *3* - ceiling level of the cavity, connecting the cavity with the outdoor air; *4* - a leakage area between the room and the air space at a given height; *5* - a given flow from the cavity to the return air duct. The first three connections are defined as equivalent leakage area (ELA) calculated with a discharge coefficient, Cd = 1 and with the flow depending on the square root of the pressure difference; therefore, they are always open and not controllable. Only the opening towards the inside can be controlled (via schedule or PI control). The AHU fan schedule controls the mechanical air flow extracted from the facade. It is also important to mention that the mechanical ventilation of the cavity only works if coupled with the HVAC system, so the air cannot be exhausted directly to the outdoors.

The ventilation strategies natively available (Fig. 3 b) in this component can cover all the needs in terms of flow path: 1) OAC naturally ventilated; 2) EA naturally ventilated; 3) IAC naturally and 4) mechanically ventilated; 5) SA naturally and 6) mechanically ventilated; 7) TB. In order to model the thermal buffer mode, at least one small leak (either toward the inside or outside) has to be modelled. However, as anticipated, the fixed-configuration feature of the component limits the model's flexibility because of two main constraints: the impossibility of controlling some opening/connection types and the impossibility of modelling all the connections at the same time (i.e., within a single simulation run it is not possible to alternate flow paths and ventilation strategies).

The solar radiation modelling through the facade is carried out in the two complex window components. The solar radiation hitting the façade is calculated from the weather file according to the solar position in the sky and the orientation of each façade. The distribution of diffuse sky radiation is computed by default using the Perez model. Afterwards, the solar radiation on an individual object, such as a window, is computed. A shading calculation model (*"Shade"*) calculates the amount of both direct and diffuse light on the receiving surface as a function of the sun's position and the presence of obstructions, including the building self-shading and the shading of neighbouring buildings. Once in the first window model, the solar radiation is geometrically distributed between the glazed and frame area. The diffused and direct radiation is computed with a layer-by-layer calculation of the multiple reflections. The transmitted solar from the first window is then distributed to the interior window with the same geometrical approach – no angular calculations are performed to calculate the solar distributions on the inner window. The whole surface of the external window is considered as the light source, not just the portion of the glass which is not shaded by external objects, and the direct and diffuse radiation are geometrically distributed to the inner glazed area and treated in the same manner as the exterior window (the two windows are modelled with two identical components). This could represent a limitation in the case of a window with a high frame ratio because the radiation entering the zone is then reduced by a geometrical factor. Once inside the zone, diffuse light is scattered uniformly while the exact target location of the direct light beam is computed.

Previous analyses have shown that the "Double Glass Façade"

Table 1

Performances of the 'Double Glass Façade' model in modelling a single-story DSF: mechanically [21] and naturally ventilated [41] – see Eq. (2) and Eq. 3

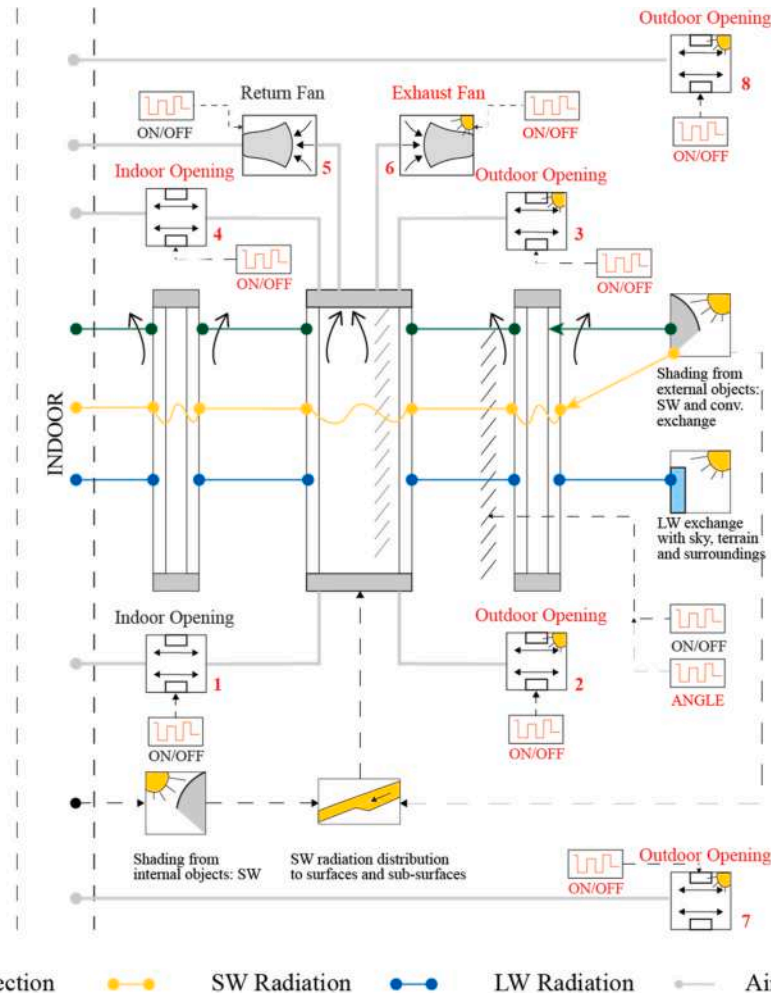| | Mechanical Ventilation | | Natural Ventilation | | | | | |
| | Exhaust Air | | Thermal Buffer | | Outdoor Air Curtain | | Supply Air | |
	MBE	RMSE	MBE	RMSE	MBE	RMSE	MBE	RMSE
Transmitted irradiance [W/m^2]	0.2	21	−0.4	14	−0.6	9.1	−2.0	15.7
Airgap Temperature [°C]	−0.3	2.6	1.4	3.7	−1.7	2.8	0.1	1.7
Surface Temperature [°C]	0.4	1.5	−0.8	1.8	0.5	1.8	0.4	1.1
Heat Flux [W/m^2]	2.6	15	N/A	N/A	−2.1	5.0	N/A	N/A

Fig. 4. Schematic view of the adaptive façade model implemented in IDA ICE based on the fully flexible DSF architecture (the model can switch among all the configurations presented in Fig. 1 within the same simulation) – in red, the newly added elements. (For interpretation of the references to colour in this figure legend, the reader is referred to the Web version of this article.)

component, in combination with the *"Detail Window Model",* is more sensitive to the parameters describing the glazing thermal and optical properties and shading optical properties than the geometrical and frame properties [40]. The performances of this component have been tested under different conditions (winter and summer) and, with different ventilation strategies (mechanical [21] and natural) in previous studies. The validation results showed good agreement with the experimental results (Table 1) for a validation covering OAC, SA, and TB configurations. The naturally ventilated cases have a similar level of error as the mechanically ventilated ones, even though the level of uncertainty is usually higher (being the buoyancy effect, the primary driver whilst in the mechanically ventilated façade, the airflow is known). In the mechanically ventilated case, the airgap temperature better agrees with the experimental data during the days when the shading was not

deployed in the cavity, while the model underestimates the peaks with the shading activated, showing a limitation of the tool in modelling the heat transfer between the shading device and the air in the cavity. The natural ventilated façade models do not show this difference. In both cases, the peaks during the daytime are underestimated. This could be linked to the uncertainty connected to the airflow estimation (size of the leaks to represent the opening, pressure loss at the level of the openings, etc.). In the thermal buffer case, the beaviour differs greatly between when the shading is drawn and when it is not. Without the shading, the model shows a slight overestimation in modelling the night-time, while the day peaks are usually well predicted; nce the higher errors occur in the part of the day where only the external and internal temperatures play a crucial role, it is possible to identify the weak link in the two-dimensionality of the component. When the shading device is
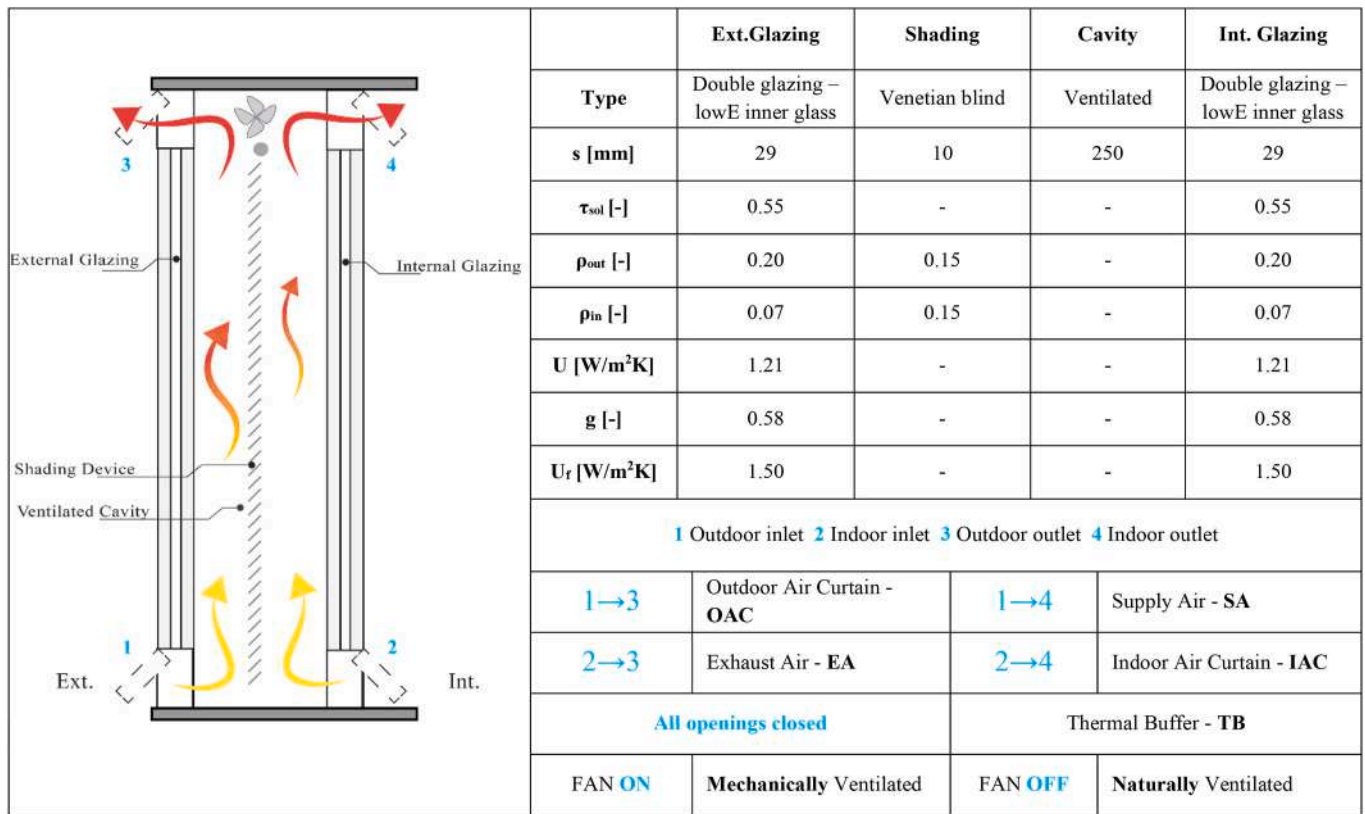
		Ext.Glazing	Shading	Cavity	Int. Glazing
	Type	Double glazing – lowE inner glass	Venetian blind	Ventilated	Double glazing – lowE inner glass
	s [mm]	29	10	250	29
	τ_{sol} [-]	0.55	-	-	0.55
	ρ_{out} [-]	0.20	0.15	-	0.20
	ρ_{in} [-]	0.07	0.15	-	0.07
	U [W/m²K]	1.21	-	-	1.21
	g [-]	0.58	-	-	0.58
	U_f [W/m²K]	1.50	-	-	1.50

1 Outdoor inlet **2** Indoor inlet **3** Outdoor outlet **4** Indoor outlet			
1→3	Outdoor Air Curtain - OAC	1→4	Supply Air - SA
2→3	Exhaust Air - EA	2→4	Indoor Air Curtain - IAC
All openings closed		Thermal Buffer - TB	
FAN ON	**Mechanically** Ventilated	FAN OFF	**Naturally** Ventilated

Fig. 5. Schematic section and glazing configuration of the DSF.

present in the cavity, the prediction of the air gap temperature worsens, leading to quite high errors.

2.3.2. Enhanced flexibility of the double glass façade model

In order to be able to control the façade in different operation modes, with full control over the different openings and maximum freedom to combine the façade with the HVAC (as schematised in Fig. 2), the air links of the *"Double Glass Façade"* component were modified (Fig. 4). First of all, to be able to control the ventilation path, operable elements were needed. This modification allows dynamic control of the connection between the cavity and the indoor and outdoor environment during the simulation runtime. A conventional model for a DSF, which is based on a concept where the airflow has a fixed path, does not require this flexibility, and therefore the link between the cavity and the two surrounding environments is defined with simple representations (leakage or free cross areas) that are not to be controlled during the simulation. To meet the operational requirements connected to the concept of the flexible DSF concept, the outside and inside connections, modelled as leaks, were replaced with operable openings (*2 and 3* - Outdoor Opening and *4* - Indoor Opening - Fig. 4). The Indoor Opening (*1*) was retained from the previously described model. Once the ventilation path is controllable, to be able to alternate between the ventilation mode (natural or mechanical), it is necessary to have a mechanical fan that extracts the air from the cavity and directs it either towards the outdoor (exhaust fan) or indoor environment (return fan). In reality, this switch could be achieved using the same fan placed at upstream of the outlet section of the DSF; however, implementing this function in BES requires the presence of two fans (due to how the elements in an airflow network are connected). The existing model presented only the Return Fan - Fig. 3-a. Therefore, an Exhaust Fan (*6* - Fig. 4) connected directly to the outdoor was added to ensure that the EA and OAC ventilation strategies were possible under a mechanical regime. Finally, to ventilate the room while by-passing the cavity (ventilated thermal buffer – TB-V), it is

necessary to exclude the cavity from the ventilation path and open all the operable openings simultaneously. As for the fan, it is impossible to change the node connection of an airflow network element (to set, for example, that the outdoor windows open towards the indoor environment rather than towards the cavity). The only way to model this configuration is to have two openings not connected to the DSF air node. Therefore, two Outdoor openings (*7 and 8*- Fig. 4) were added on the same surface hosting the flexible DSF.

The openings, fans, and shading devices were connected to a controller (*[ON/OFF]* - Fig. 4). In order to be able to control the angle of the slats of the shading device, a controller (*[ANGLE]* - Fig. 4) was connected to the shading device of the external window. The fans work as an idealised exhaust terminal, which works as an ON/OFF fan controlled by a schedule. If the fan is set to OFF, the fan behaves as a leak and adopts the nominal minimum airflow rate (this value cannot be set to zero, but since the field accepts rational numbers, it was possible to set this variable to a value very close to zero). The infiltrations were modelled in the opening components, which, when closed, are still modelled as a two-way flow opening with a reduced width.

Compared to the standard component described in 2.2.1, the modifications implemented in the new model have introduced the possibility of controlling the façade with the five different air paths available (including switching between naturally and mechanically ventilated mode) and, therefore, enhanced the DSF model's flexibility. The controllers can be connected to a schedule or implemented with an external control logic that accounts for the ambient conditions (radiation, temperature, etc.).

Nevertheless, some of the limitations of the original model persist. The unique value of the airgap temperature and the modelling of the shading device as part of the external window are not easily addressable without changing the equations inside of the component. On the other hand, the geometrical distribution of the solar radiation and the two-dimensional heat exchange can be addressed, if the dedicated case
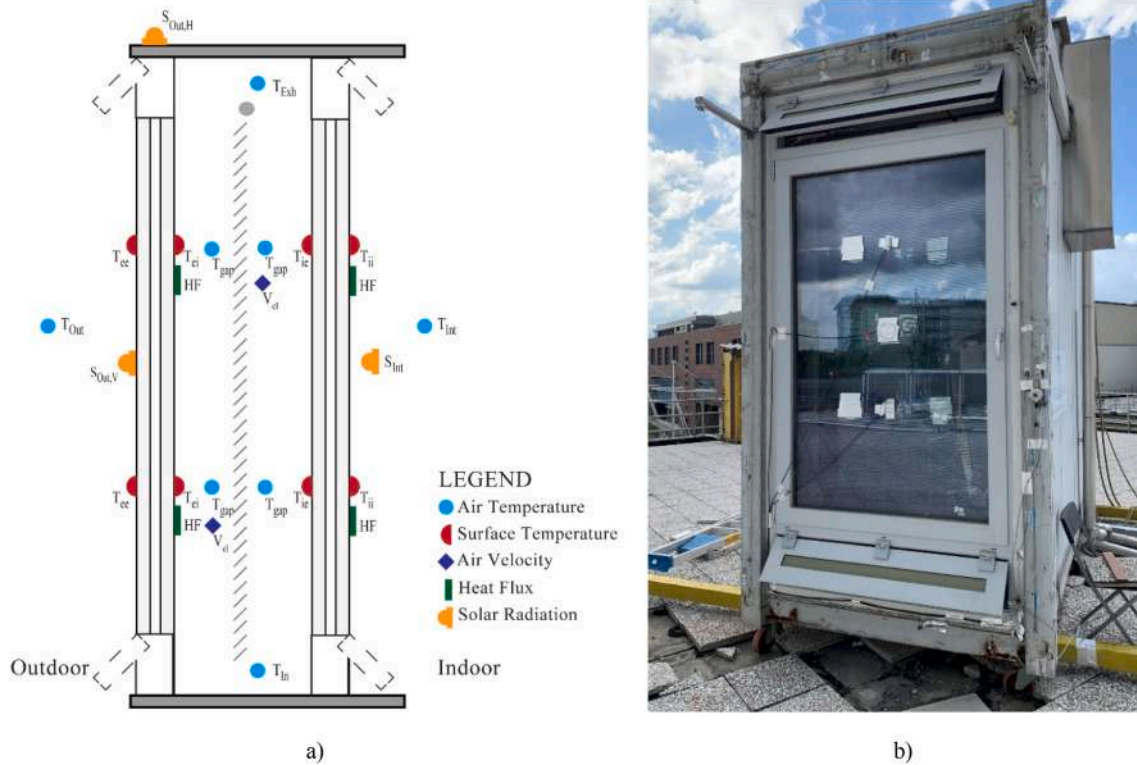
Fig. 6. Sensor a) scheme and b) instalment on the experiment facility.

requires so, with some work-around within the IDA ICE model, as explained in section 4.1, where the application of this model to model an existing DSF mock-up will be later presented.

3. Experimental set-up and data collection for model validation

The validation of the performance of the modified "Double Glass Façade" component to address the simulation needs of the flexible DSF concept was carried out by comparing simulation results with experimental data. Experimental data were collected using a single-storey DSF mock-up that was run in a fully dynamic way (i.e., changing the operational configuration of the façade), as explained in the following sections. The experimental set-up is described in 3.1. The control strategies adopted during the experimental campaign to collect data under very different operational modes are presented in 3.2, whilst the boundary conditions for those selected weeks are in 3.3.

3.1. Experimental set-up

The DSF mock-up was installed in an outdoor test-cell facility in a temperate sub-continental climate in Torino, Italy (45° N latitude). The test-cell was located on a flat roof of a building on the campus of Politecnico di Torino, not shaded by the surrounding buildings and had a (nearly perfect) South exposure. The test cell room had internal dimensions of 1.60 m (façade test rig) x 3.6 m (depth) and 3.0 m (height). These dimensions are derived from the IEA-SHC TASK 27 specifications for typical dimensions of spaces behind façade modules used in office buildings. The test cell's indoor air conditions were controlled with a full-air system that can maintain the room's indoor air temperature between 20 °C and 26 °C with a single set-point or the test cell can be left uncontrolled for free-floating tests.

The façade used for the validation of the flexible model had dimensions of 1.60 m (width) and 2.90 m (height, including the opaque bottom/top inlet/exhaust section), and a ventilated cavity of 0.25 m (depth) and hosted a highly reflective venetian blind as a shading device

located at the centre of the cavity (Fig. 5). The airflow entered the ventilated cavity from the pivoting openings at the bottom of the façade and exited it from the cavity top openings. The openings towards the inside or outside are chosen depending on the operational mode. If the façade was mechanically ventilated, four fans were activated at the top of the glazed cavity, upstream of the outlet section, and their total nominal volumetric airflow was 15 l/s. Both skins of the DSF were made of an insulated glazed unit with two glass panes with a low-e coating. Details of the thermal and optical properties of the components of the DSF mock-up are given in Fig. 5.

The test cell and the DSF mock-up (Fig. 6) were equipped with a wide range of sensors (resistance temperature detectors for air temperatures, thermocouples for surface temperature measurements, heat flux meter sensors, anemometers for the airspeed, and pyranometers both inside and outside) to record the thermophysical and optical processes occurring in the DSF. Temperature and heat flux sensors were placed at two height levels, both inside and outside of the façade, measuring: the surface temperature of the interior glazing and the exterior glazing (both towards the indoor and the cavity); the temperature of the air in the cavity both in front and behind the shading (when present); the inlet and outlet cavity-air temperature; the frame temperature; the heat flux exchanged at the indoor surface of the glazing. Thermocouples and heat flux meters directly exposed to solar radiation were shielded with highly reflecting aluminium foils to reduce the influence of solar irradiance on the measured physical quantity, following best practices established in the literature [42]. Though the mock-up's cavity also hosted hot-wire anemometers, air speed readings in the cavity are not always reliable, as values can fall below the lower threshold of the sensors. Generally speaking, a continuous characterisation of the air velocity in the cavity is a challenging task [36], so we decided not to employ the air speed values measured by the hot-wire anemometers in the validation process.

The outdoor solar irradiance was measured horizontally and vertically, employing two pyranometers. The solar irradiance transmitted through the DSF was measured, on the vertical plane, with an additional pyranometer installed right next to the inner skin of the DSF. The wind
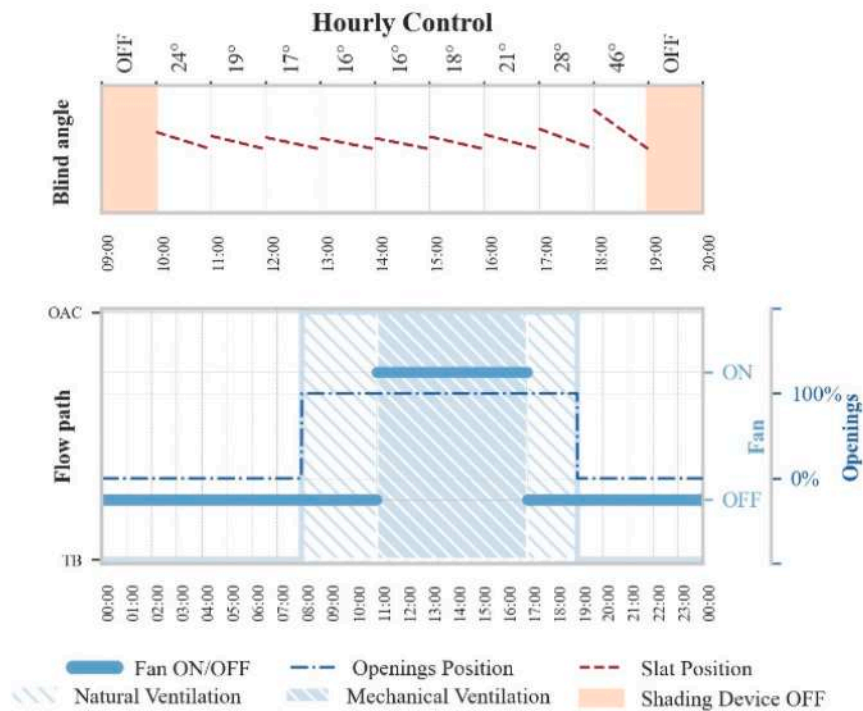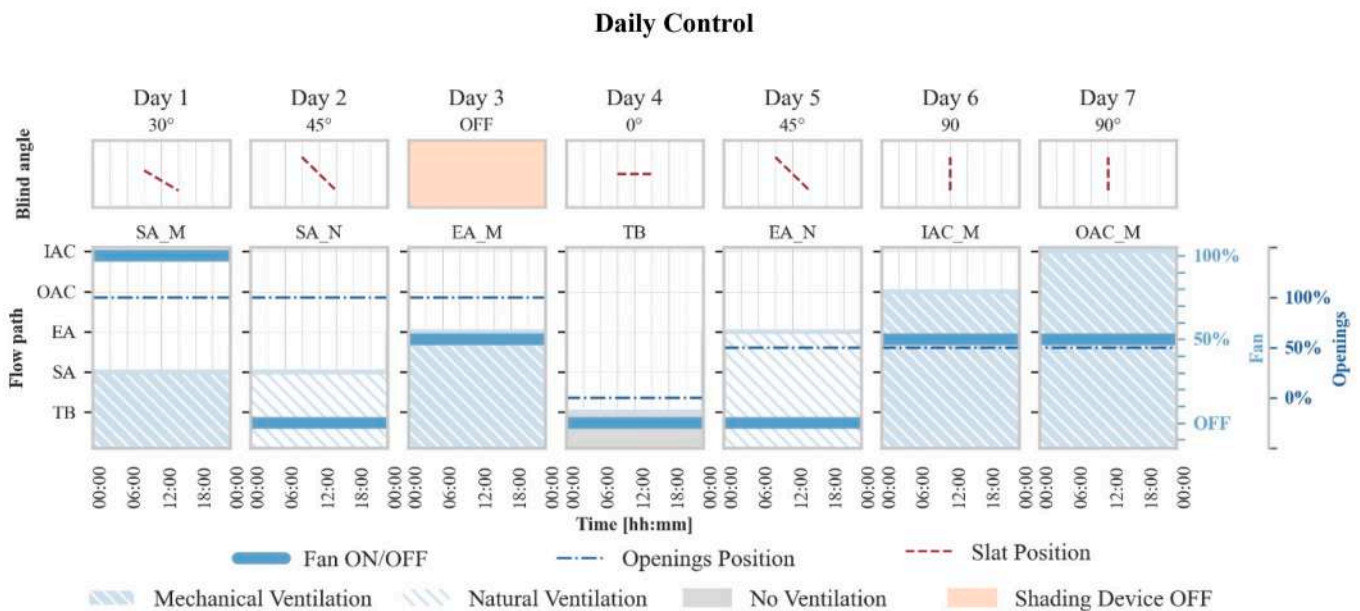
Fig. 7. Control strategies applied in the two analysed periods a) Hourly Control – applied for every day of the week and b) Daily Control.

speed and wind direction were also recorded. The test cell was also equipped with RTD (PT100) sensors to record the indoor air temperature values. The cell surfaces' temperatures were measured by thermocouples in parallel, so only the mean value for the whole set of surfaces (other than the DSF mock-up) surrounding the indoor air volume was registered.

All the data were acquired with a 1 min resolution. The measurement

accuracies for the entire measurement chain, after calibration and verification, were: ± 0.3 °C for the resistance temperature detectors, ± 0.5 °C for thermocouples and $\pm 5\%$ for the flux meters and pyranometers.
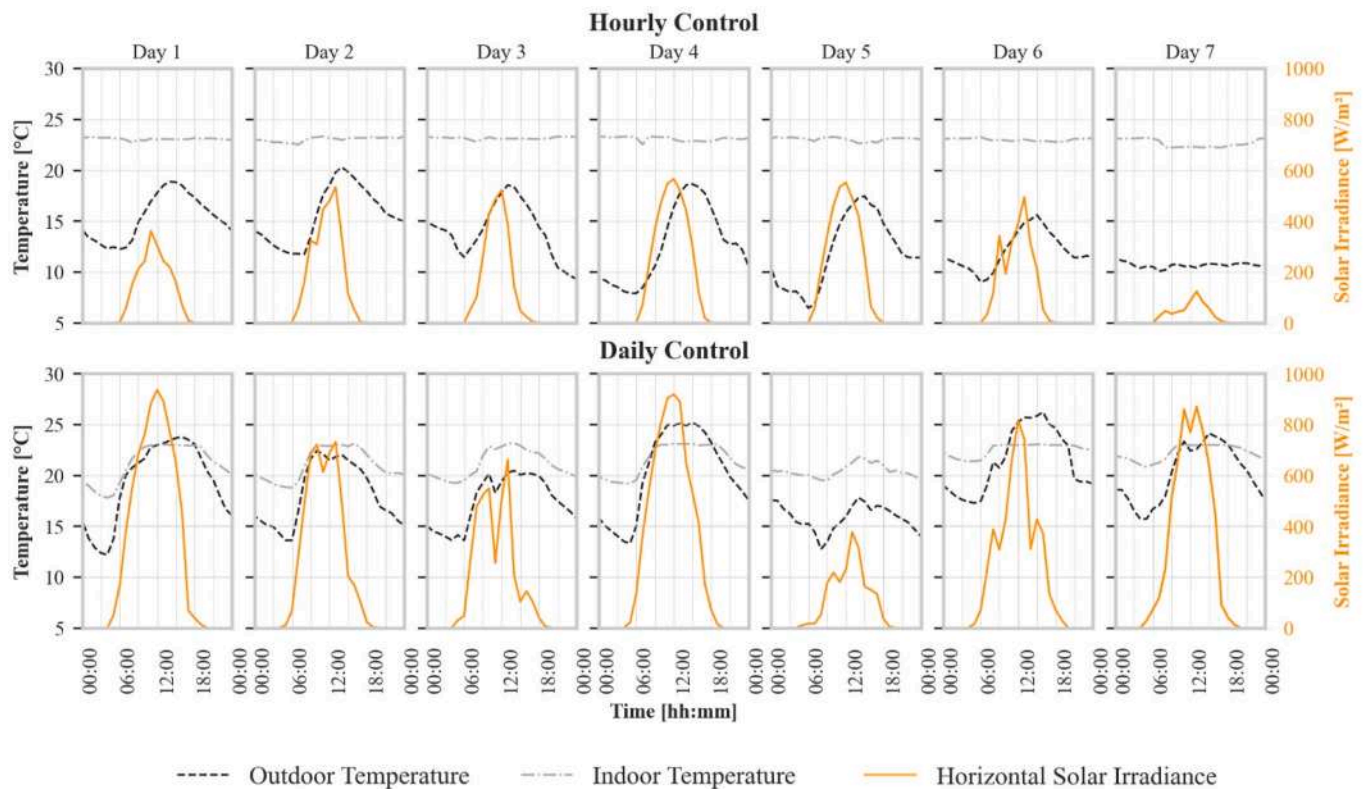
Fig. 8. Time profile of the outdoor and indoor air temperature [°C] and horizontal global solar irradiance [W/m2] for the two modelling periods: a) Hourly Control and b) Daily Control.

3.2. DSF's control under experiments for model validation

The data set chosen for the validation is relative to two different periods of measurement when the operational modes of the façade, managed by its onboard controller, were as follows: in the first period (called *Hourly Control*), the façade configuration was changed every hour using a pre-defined, scheduled-based, control; in the second period (*Daily Control*), the configuration of the façade was changed every day by exploring a wider range of combinations of all the possible configurations that the façade can assume, but the configuration of the façade was fixed for 24 h. By designing the validation process to include these two periods, we aimed to assess the numerical model's ability to replicate both fast-time processes and more long-term dynamics and simulate an extensive range of operational conditions. Overall, both mechanical and natural ventilation were employed, the shading device was deployed or retracted, and the slats of the venetian blinds were changed every hour by a few degrees to direct solar radiation cut-off (for the Hourly Control only), and different ventilation paths were employed (see Fig. 5). Fig. 7 shows the details of the operational conditions of the façade applied in each period.

3.3. Boundary conditions for validation

Fig. 8 shows the main boundary conditions (outdoor and indoor air temperature and global irradiance on the horizontal plane) for two selected periods, equivalent to two weeks. In the first period, the indoor temperature was controlled and set to 23 °C, while in the second one, the indoor air temperature of the room was left free to float between 18 °C and 23 °C to increase the range of boundary conditions employed in the validation process.

The experimental data of the boundary conditions during the experiments were used to construct a customised 10 min-resolution weather data file. The measurements available to create the customised

weather data files included the global solar irradiance data on the horizontal plane, the outdoor air temperature and the wind direction and velocity. The required weather data are, in addition to the outdoor dry bulb temperature, the direct beam and diffuse horizontal solar irradiance, the cloud cover fraction of the sky, and the relative humidity of the air. The beam and diffuse components of the solar radiation were calculated using the ENGERER2 separation model [43] with a 1-min parametrisation. The source of the relative humidity was the official weather station of Politecnico di Torino, installed on campus, relatively near the testing site, and the source of the cloudiness factors was the climate reanalysis ERA5 [44]. The different time resolution of each dataset was set to 10 min to create a unique weather file.

A sensitivity analysis was carried out to verify that the uncertainty in the decomposition of the solar irradiance in the direct and diffuse components (which were not directly measured) showed little impact on the validation process results. Furthermore, since the measurement of the global irradiance on the vertical (façade) plane was available from the experimental dataset, the goodness of the decomposition procedure adopted was verified by comparing the numerically calculated global solar irradiance on the vertical (façade) plane with the measured value for the same quantity.

The measured indoor air temperature and the test cell's opaque surfaces' temperatures were adopted in the simulation to ensure identical boundary conditions to the experiments as shown in Fig. 8, and better described in Section 4.2.

4. Numerical model validation: methods, results, and discussion

4.1. Implementation of the façade prototype in IDA-ICE for simulation of the experimental campaign

The numerical representation of the DSF mock-up was developed, modelling the cavity as a ventilated wall because of the geometry of the

façade, characterised by a high frame ratio. This choice had other implications on how the inner face had to be modelled, which are discussed later in this section.

To replicate the operational strategies of the façade used during the experimental campaign, each leak was replaced with a two-way flow vertical opening, and an exhaust fan was added. Each opening was a 1.4 m wide and 0.30 m high top-hinged window. The maximum opening angle was 45%. In order to reflect this geometry, the opening width was calculated using Equation 14 of the TRNFLOW manual [45]. A schedule controlled the openings, the fans and the shading device. The fans worked as an idealised exhaust terminal, which worked as an ON/OFF fan controlled by a schedule. If the fan was set to OFF, the fan behaved as a leak and adopted the nominal minimum airflow rate. This value cannot be set to zero, but it was set to a value close to it (10^{-4} l/s). The effect of infiltration was included in the openings' representation. When closed, openings are still modelled as a two-way flow section with a reduced width. A leakage coefficient of 10^{-4} was considered for each opening to represent the air infiltration from the closed openings.

As mentioned earlier, the ventilated cavity was modelled as a *"ventilated wall"*. This choice was made because such an approach allows the modeller to modify the solar radiation distribution onto the inner glazing once it goes through the outer one. By default, the total transmitted solar irradiance is evenly distributed to the inner glazing and frame area, independently from the incident angle or the view factor between the two glazing. The frame ratio of the case study was around 60%; thus, only 40% of the solar radiation entering the cavity was transmitted to the inner glazing, resulting in a much lower irradiance transmitted towards the inside room.

To overcome this limitation, the internal facade was modelled as a smaller window –of the same dimension as the glazed area of the internal glazing – with a 0.1% of frame; the wall to which the window belongs was modelled with the same U-value of the aluminium frame, and the external skin was modelled as a ventilated wall, occupying the whole exposed façade. In the external window, no changes to the geometry were made. When adopting this modelling strategy, the ratio of solar radiation hitting the inner glazing was changed to 70% - and 30% distributed to the wall frame; in this way, a more realistic transmitted solar irradiance was calculated, and the solar heat absorbed by the inner frame was accounted for, as well as the heat loss through the external frame.

No enclosing elements around the cavity were considered in the calculation, except for the façade elements (glazing, frames, shading) parallel to the façade [46]. To consider the heat transfer through the sides of the ventilated cavity, the U-value of the external frame was set to an equivalent U-value (3 W/(m²K)) which accounted for the external frame itself, the thermal bridges, and the side surfaces of the cavity.

The shading layer was set as part of the exterior window, and it was modelled as an interior venetian blind. Its distance was defined as measured from the external skin and set as in the experimental set-up. A schedule controlled the shading's presence inside the cavity and the angle of the blinds.

4.2. Methods and procedure for experimental validation

The goal of the validation procedure was to check to what extent the modified *"Double Glass Façade"* model could replicate the thermo-physical and optical behaviour of the façade mock-up. For this reason, the focus of the validation was placed on the DSF modelling alone and not on the combination DSF and room (or test cell). This means that each surface of the virtual room and the indoor air node temperature of the virtual room were given values through schedules created using the available experimental data. The geometry of the virtual room replicated the geometry of the test cell where experiments were carried out and used the same dimensions as the physical room. This strategy allowed us to replicate the indoor and outdoor boundary conditions surrounding the DSF, thus focusing the validation on the DSF models'

performance since all the other possible uncertainties in the simulation tools linked to the environments surrounding the DSF were removed. Alternative approaches such as a validation using room-level quantities (e.g. indoor air temperature or energy/power required to climatise the test cell) would likely lead to much higher uncertainty because more unknowns and more simulation routines are involved, and to the impossibility of assigning potential discrepancies to the different routines of the tool (e.g. whether a discrepancy is due to insufficient performance of the routine under test or is due to other routines used to model other components in the room, or due to unknown in the modelling of the other components of the room).

This validation approach adopted in this study, which is commonly exploited for validating individual simulation routines of building envelope systems, has however a disadvantage in the impossibility of finding literature reference values to define when the simulation output is "well enough" to consider the model validated. For example, the ASHRAE Guideline 14 [47] defines model calibration criteria that can be used to check the reliability of a simulation model to replicate the energy use in the whole building. However, when the parameters used in the validation are "detailed" physical quantities (as explained in the following paragraphs), there are no reference literature values that can be used for this purpose; it is left to the sensitivity of the researcher to decide if the level of accuracy reached by the numerical simulation is deemed sufficient.

Simulations were then run using the custom built weather data file and all the experimental data that could represent the boundary conditions around the DSF mock-up. The maximum simulation time step (IDA ICE adopts a dynamic simulation time-step) was set to 10 min, which means that if the simulation converged sooner, the time step was lower. The numerical outputs were extracted and sampled with a time-step of 10 min. The following (simulated) physical quantities were obtained:

- the transmitted solar irradiance through the innermost windowpane of the DSF [W/m²];
- the air temperature of the cavity [°C];
- the surface temperature of the interior surface of the interior glazing [°C];
- the heat flux on the interior surface of the interior glazing [W/m²];

These quantities were compared with the following experimental data:

- the transmitted solar irradiance through the entire DSF structure, measured on the vertical plane [W/m²].
- the averaged air temperature of the cavity (average value of 4 sensors) [°C];
- the averaged surface temperature of the interior surface of the interior glazing (2 sensors) [°C];
- the (average) specific heat flux (i.e., the sum of the convective heat flux exchanged between the surface of the inner skin and the indoor air and the radiative heat flux in the longwave infrared region exchanged between the surface of the inner skin and the surfaces of the room behind the DSF) (2 sensors) [W/m²];

Moreover, an indicator called "total transmitted energy", which gives the energy crossing the façade (normalised for per square meter of façade), expressed in [Wh/m²], was derived using the heat flux exchanged at the indoor-facing surface of the DSF and the transmitted solar radiation as shown in Eq. (1). The total transmitted energy can be calculated for a single hour, a period of 24 h (total daily energy) or for a longer period (e.g., one week). The aim of this performance metric, in a validation perspective, is to assess how well the entire room load due to the façade is replicated by the simulation environment, regardless of the more or less perfect match between individual physical quantities. These values were calculated both for the experimental and the simulated data

for both periods analysed for both the overall period (7 days for the Hourly Control period and 7 days for the Daily Control period) and for each day.

$$E_{tot} = \sum_{i=1}^{t} \left(Q_{HF}^{+} - Q_{HF}^{-} + Q_{SOL} \right) \qquad (1)$$

where.

E_{tot} is the total energy for the t interval
Q_{HF}^{+} is the positive flux entering the room for a single hour;
Q_{HF}^{-} is the negative flux entering the room for a single hour;
Q_{SOL} is the solar flux entering the room for a single hour;
t number of hours for the analysed period.

The model validation was carried out through combined qualitative and quantitative analyses. This approach allows quantifying the performance and understanding the different observed behaviours. The time profiles of the thermophysical quantities identified in the previous section were helpful in supporting the qualitative (and explanatory) assessment. The quantification of the mismatch between the experimental data and the numerical data was assessed through the calculation of two commonly used statistical indicators, as described in the following equations: the Root Mean Square Error (RMSE) (Eq. (2)) and the Mean Bias Error MBE (Eq. (4)). The normalised values of these indicators were calculated for evaluating the fitness of the models in predicting the total energy crossing the DSF: Coefficient of Variation of the Root Mean Square Error [CV(RMSE)] (Eq. (3)) and the Normalised Mean Bias Error (NMBE) (Eq. (5)).

$$RMSE = \sqrt{\frac{\sum_{i=1}^{n} (P_i - M_i)^2}{n}} \qquad (2)$$

$$CV(RMSE) = \frac{RMSE}{\overline{y}} \bullet 100 \qquad (3)$$

$$MBE = \frac{\sum_{i=1}^{n} (P_i - M_i)}{n} \qquad (4)$$

$$NMBE = \frac{MBE}{\overline{y}} \bullet 100 \qquad (5)$$

where.

P_i – predicted value by the simulation;
M_i – measured value at one point;
n – total number of measurements;
$\overline{y}$ – mean value of the measured values.

When it comes to the calculation of CV(RMSE) for the total energy indicator, this statistical indicator can be performed using different integration time to calculate the total energy, i.e. CV(RMSE)$_{1H}$ if the total energy is calculated hour by hour and then the experimental value is compared to the simulated value; CV(RMSE)$_{24H}$ if the total energy is calculated for an entire day and then this experimental datum is compared with the simulated one. Clearly, because of how NMBE is defined, there is no difference in the value of this indicator for different integration periods of the total energy quantity.

The set of statistical indicators adopted in this study had been used in previous model validation dealing with some specific configurations of DSF [41] activities that can be used for benchmarking the performance of the flexible model – i.e., to assess whether the performance of the developed numerical model that replicates the flexible DSF is at least equal to that of the "basic" DSF model of IDA ICE. For this purpose, both the experimental and the simulated data were averaged to hourly values.

4.3. Model performance analysis

4.3.1. Overview and prediction of total transmitted energy

This section gives an overview of the flexible model's performance for the physical quantities employed in the validation process. As previously mentioned, the transmitted solar irradiance, airgap and surface temperature, and heat flux transmitted were chosen for this comparison to assess the model reliability for detailed thermophysical process simulation, while the total energy indicator was used to assess the accuracy of the simulation to replicate the overall impact of the façade system on the room thermal load. As mentioned, the simulated data were collected for seven days for both the hourly and daily controlled periods. The statistical indicators were calculated for the entire simulation periods of the Hourly Control and Daily Control (Table 2) and in detail (Table 3) for each day of the Daily Control.

The distribution of the errors for the different ventilation modes and the different variables shown in Fig. 9-a highlights how, for most of the configurations, the predictions are very similar to the measured values, with the supply air configurations having the biggest overestimation of the airgap temperature and heat flux, while the thermal buffer underestimates the heat flux. As shown in Fig. 9-b, the surface temperature has the lowest error (RMSE) for all the configurations, while the heat flux has the highest one. The simulation error of the airgap temperature value is highest during the mechanical supply configuration. A more detailed analysis of each of the four thermophysical variables is given in the following sections.

When comparing the total energy crossing the façade, which includes the energy gained and lost by the DSF due to all the heat transfer mechanisms, the values predicted during the Daily Control showed a better agreement with the measured data than the Hourly Control period (Table 4) when the analysis is done comparing total energy values hour by hour using the CV(RMSE)$_{1H}$. The cause of this is linked to the dynamicity of the façade (in terms of ventilation strategy and shading position) which is likely more emphasised during the hourly controlled period. This difference disappeared when comparing experimental and simulated daily total energy values (CV(RMSE)$_{24H}$). By using this metric, the daily variations seen when analysing the dynamic parameters are no longer distinguishable and this shows that the influence of the discrepancy on an hourly basis has very little influence on the overall energy balance. When the focus is placed on each day of the Daily Control the prediction of the total energy values for the façade configurations operated under naturally driven ventilation had a higher error compared to the cases when the ventilation in the cavity was mechanically driven. Nonetheless, the overall assessment demonstrated that when used to assess the overall performance in terms of total energy crossing the façade for a long enough period of time (as typically done through BES tools), the flexible DSF model gives estimations that are close to the measured values, with MBE in the range of 5–15%.

In summary, the general assessment covering the four detailed thermophysical quantities and the total energy parameter demonstrated the model's ability to predict the behaviour of the flexible DSF that is characterised by fast changes in the schedule for both the ventilation
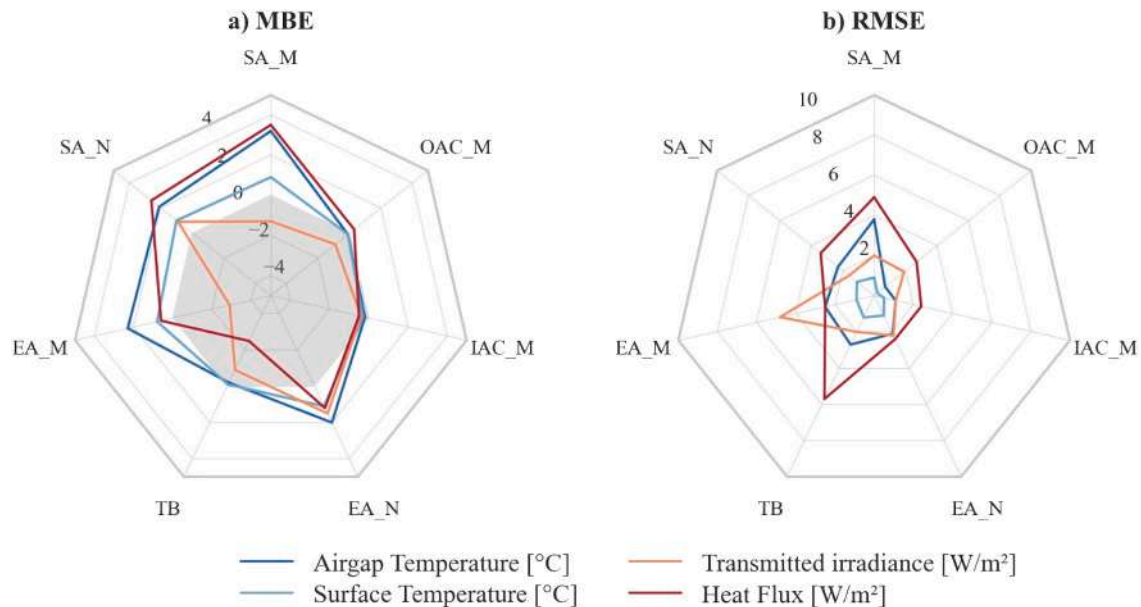
Table 2
MBE and RMSE values calculated for the model run adopting the Hourly Control and the Daily Control.

	Hourly Control		Daily Control	
	MBE	RMSE	MBE	RMSE
Airgap Temperature [°C]	1.5	2.2	1.3	2.4
Surface Temperature [°C]	−0.2	0.3	0.5	0.9
Transmitted solar irradiance [W/m²]	2.0	4.8	−0.6	2.5
Surface Heat flux [W/m²]	3.9	4.7	0.7	3.7

Table 3

Detail of the MBE and RMSE calculated for each ventilation strategy adopted in the Daily Control.

Ventilation path	Day 1		Day 2		Day 3		Day 4		Day 5		Day 6		Day 7	
	SA_M		SA_N		EA_M		TB		EA_N		IAC_M		OAC_M	
Opening %	100		100		100		0		50		50		50	
Fan %	100		OFF		50		OFF		OFF		50		50	
Shading device	30°		45°		OFF		0°		45°		90°		90°	
	MBE	RMSE	MBE	RMSE	MBE	RMSE	MBE	RMSE	MBE	RMSE	MBE	RMSE	MBE	RMSE
Airgap Temperature [°C]	3.2	3.8	2.1	2.3	2.3	2.5	−0.2	2.7	2.0	2.1	−0.2	1.1	−0.1	0.7
Surface Temperature [°C]	0.9	0.9	1.0	1.1	0.8	0.9	−0.1	1.2	1.1	1.1	−0.3	0.5	−0.1	0.2
Transmitted solar irradiance [W/m^2]	−1.3	2.0	0.9	1.6	−2.9	4.8	−0.9	2	1.5	2.2	−0.4	1.1	−0.9	1.9
Surface Heat flux [W/m^2]	3.5	4.9	2.6	3.4	0.6	2.5	−2.5	5.7	1.2	2.4	−0.5	2.4	0.3	2.7

Fig. 9. Statistical indicators a) MBE and b) RMSE distribution for each configuration tested during the Daily Control.

strategy and the solar control. The flexible model shows similar results compared to the base model runs (Table 1); the statistical values show lower or similar results for most variables. More details on the prediction of the four thermophysical quantities are presented in the following sections.

4.3.2. Prediction of transmitted solar irradiance

During the Hourly Control (Fig. 10), the control on the shading device and the actuator on the blind angle replicated the profiles the schedule gave. The simulation slightly overpredicted the transmitted solar, particularly during the first hours of mostly sunny days. The error during the sunny days was circa 10 W/m^2, and it was mainly linked to the uncertainty of the exact position that the blind acquired during the

selected week. The angle settings were recorded from the blind controller, but the exact angle adopted was not measured. With just a little adjustment of 5°, the errors were reduced by half, in line with the error magnitude of the Daily Control. During these days (Fig. 11), the time profile showed a good agreement with the measurements, both with the shading device activated and without it. It is also not fully possible to exclude that, for particular angles, due to the geometrical relationship between the sun position, the blinds, and the pyranometer, the sensor was partially shaded, and thus the reading obtained by this device might not have been fully representative of the average value across the whole glazed area (which is instead the value obtained by the simulation). This effect could explain why, in cases where no shading devices were deployed (Fig. 11 - Day 3), i.e., when the sensor's reading

Table 4

Daily total transmitted energy performances and statistical values (NMBE and CV(RMSE)) calculated for the Hourly Control and Daily Control (7 days period) and for each day of the Daily Control (24H period).

	Hourly Control	Daily Control	Day 1	Day 2	Day 3	Day 4	Day 5	Day 6	Day 7
			SA_M	SA_N	EA_M	TB	EA_N	IAC_M	OAC_M
Measured total energy [Wh/m^2]	1766	1766	253	181	466	461	64	167	184
Predicted total energy [Wh/m^2]	1858	1524	253	198	360	343	90	134	146
NMBE [%]	5	−14	−0	9	−23	−26	41	−20	−21
CV(RMSE)$_{1H}$ [%]	75	42	35	53	31	37	110	32	36
CV(RMSE)$_{24H}$ [%]	26	25	N/A	N/A	N/A	N/A	N/A	N/A	N/A

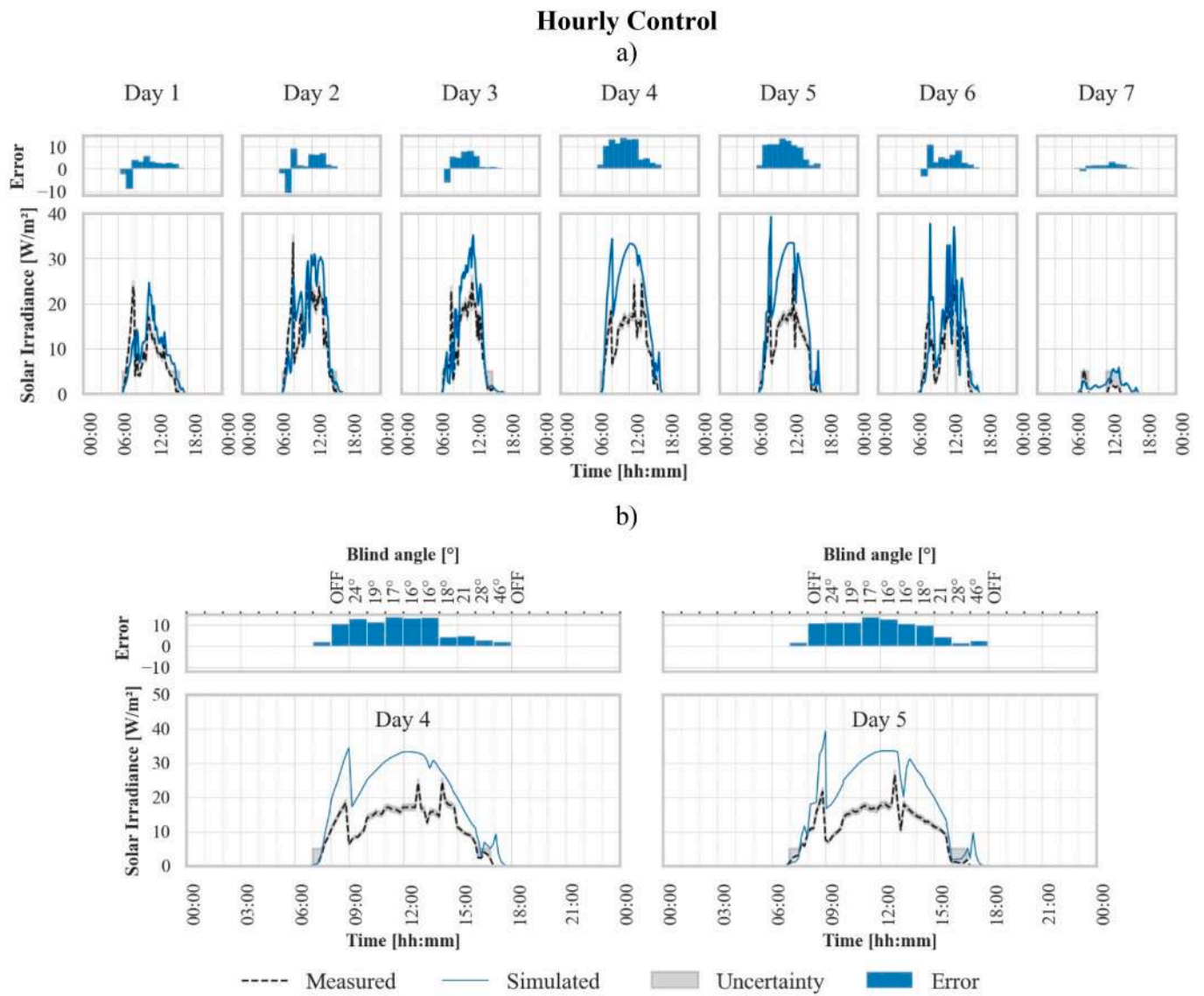## Hourly Control

a)

b)

Fig. 10. a) Time profile of the transmitted solar irradiance for the hourly controlled days; b) detailed view of Day 4 and 5. The error is expressed in [W/m²]. The uncertainty band is calculated as ±5% of the measured values.
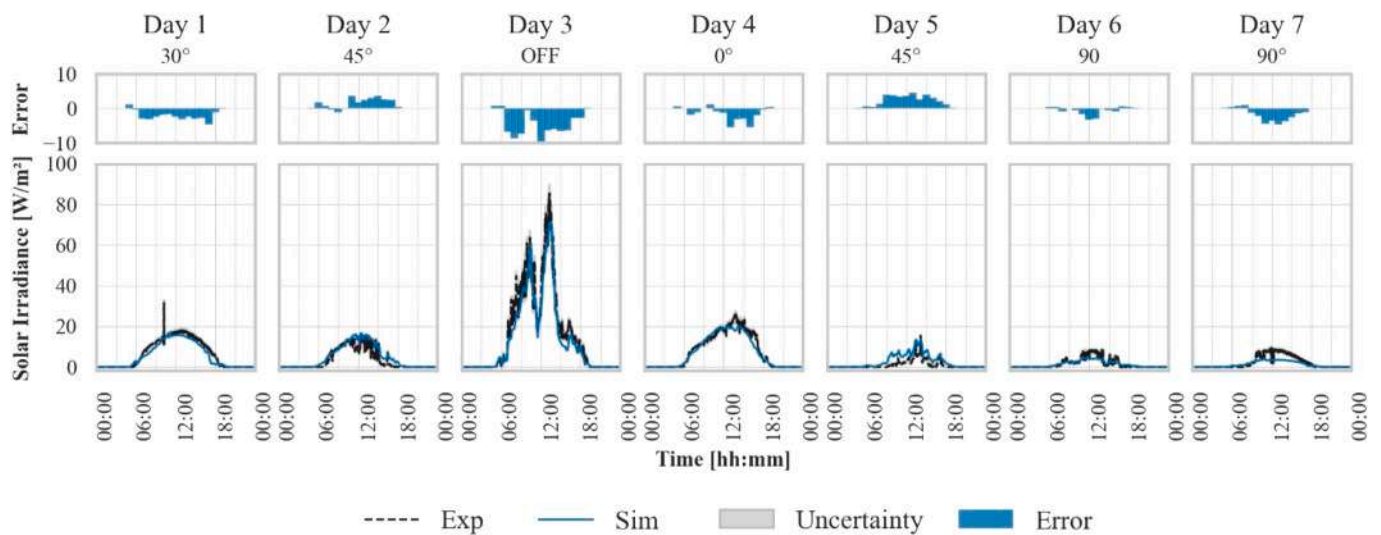

Fig. 11. Time profile of the transmitted solar irradiance for the daily controlled days. The error is expressed in [W/m²]. The uncertainty band is calculated as ±5% of the measured values.
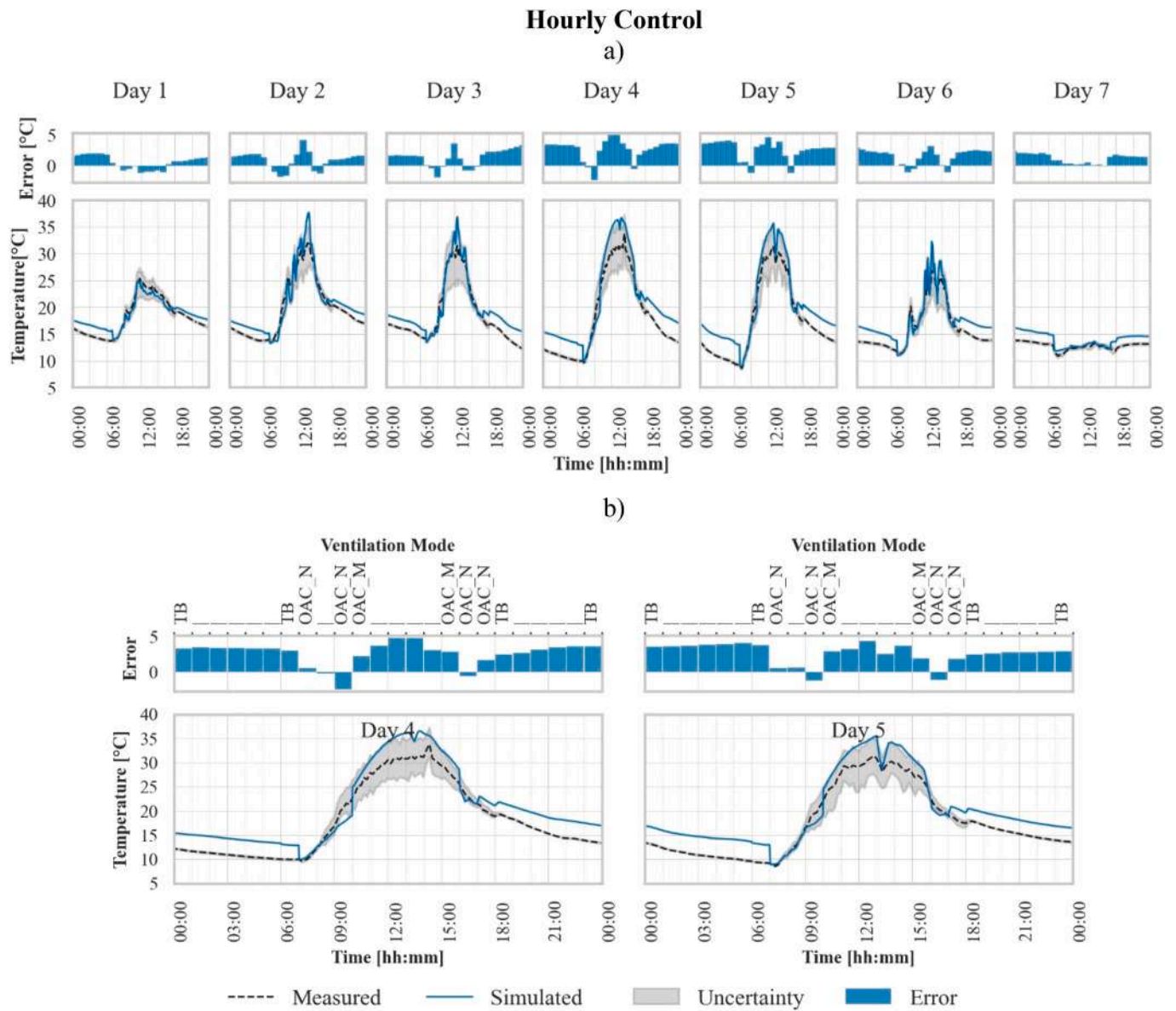
Fig. 12. a) Time profile of the air gap temperature for the hourly controlled days; b) detailed view of Day 4 and 5. The error is expressed in [°C]. The uncertainty band shows the experimental values measured by the sensors in the cavity placed at two different heights in the cavity.

cannot be affected by unwanted local shading phenomena due to the blind structure, the match between the experiment and simulation was very high (considering the higher value of transmitted irradiance).

4.3.3. Prediction of air gap temperature

The airgap temperature prediction varied according to the ventilation strategy adopted. During the Hourly Control (Fig. 12), the façade adopted the thermal buffer mode, the naturally ventilated outdoor air curtain mode and the mechanically ventilated outdoor air curtain mode. Among these, it is possible to notice that when the façade was naturally ventilated, the model's predictions were lower than the measured values. On the other end, the model overestimated the temperature inside the cavity when the ventilation switched to the mechanical mode and during the night-time when all the openings were closed. This latter

effect could be connected to the two-dimensional approximation done in the component; the heat losses through the external frame of the cavity might not be high enough to replicate the actual heat losses through the sidewalls of the cavity.

This trend was confirmed during the daily controlled period (Fig. 13). Generally, there was an overestimation of the air gap temperature during the days when the façade was mechanically ventilated, and this overestimation was reduced when the façade was run with natural ventilation. Looking at the trends, we can see that the model well depicted this quantity's dynamics and variation, with the highest error being around 5 °C. The thermal buffer mode showed a slight underprediction during the day and, as during the hourly controlled period, a slight overprediction during the night-time. The tool was able to replicate the high temperature reached in the gap (around 50 °C) during the
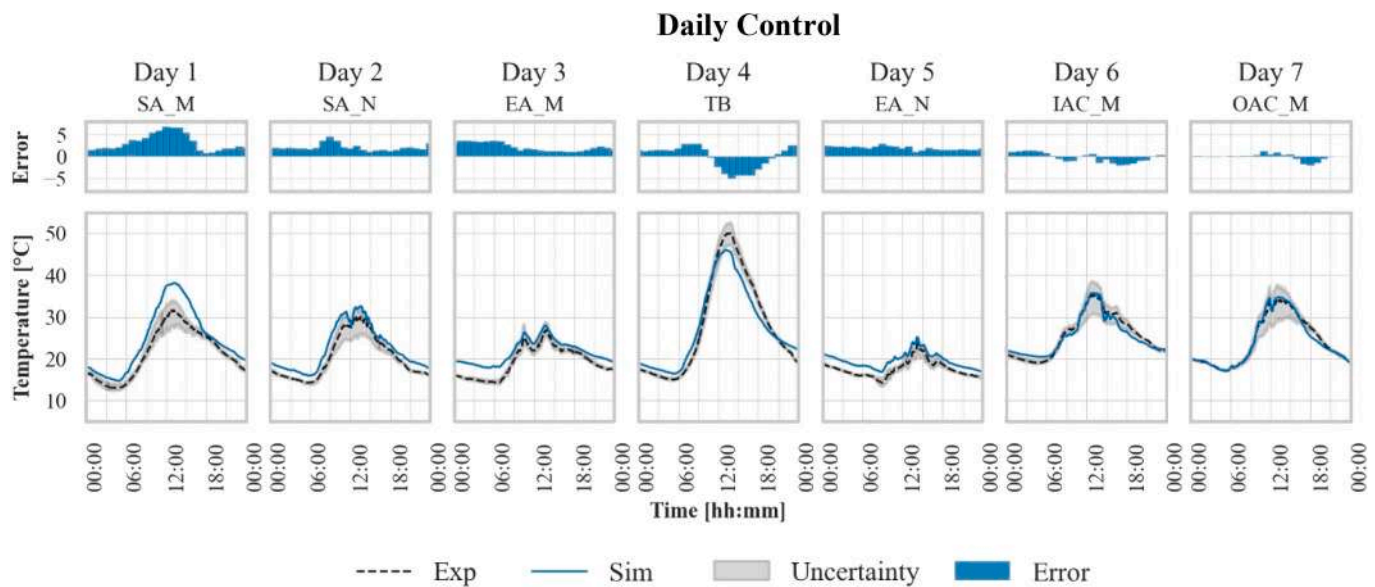
Daily Control

Fig. 13. Time profile of the air gap temperature for the daily controlled days. The error is expressed in [°C]. The uncertainty band shows the experimental values measured by the sensors in the cavity placed at two different heights in the cavity.

experiment: the shading device played a crucial role in absorbing the solar irradiance and transferring this energy quantity to the air via convection. During the night-time, the temperature was slightly over-predicted (around 1 °C), but it performed better than the night-time of the hourly controlled days due to the more negligible difference between the cavity and outdoor temperature. Similarl to what happens in the night-time of the hourly controlled period, this effect can probably be linked to the approximation of modelling the gap in two dimensions (the sides of the cavity are not modelled, and are thus not exposed to outdoor air). During Day 4 and 5, in particular, the outdoor temperature fell below 10 °C (see Fig. 8), and from the experimental data, it was possible to see that there was a heat loss from the cavity towards the outside, which the simulation cannot depict.

When the façade was run in supply air mode with the fan ON, the predicted airgap temperature values were higher than the measured data. This phenomenon could be due to an underestimation of the supplied airflow in the experimental data; as also visible in the Hourly Control data, when the openings were at 100% of their open area, the gap temperature was underestimated by around 5 °C. It could be that, due to how the experiment was run, the natural airflow was higher than the flow generated by the fan alone (which is used as input data), therefore reducing the cavity temperature more than predicted.

4.3.4. Prediction of surface temperature (of the inner skin)

The prediction of the indoor surface temperature was generally accurate in all the configurations, except for the thermal buffer mode. The surface temperature is affected by the room conditions and less affected by the cavity temperature, especially considering the insulated glazed unit of the inner skin. Therefore, if the simulated temperature of the air gap was a few degrees lower than the actual one, this led to a less significant (or none) impact on the inner face of the DSF. Most of the time, the predicted values were within the range of measure values from the experimental set-up. As shown in [21], the possibility given by IDA ICE of modelling the capacitive node in the glass led to no shifting in the surface temperature of the inner glass, an effect that is sometimes seen in

other BES tools. The time profiles of the hourly controlled period (Fig. 14) showed simulated values with an error smaller than 1 °C, and the highest errors were only seen when there was a peak in the experimental data (corresponding to the peak of transmitted solar radiation in the morning).

The results of this parameter showed a very good approximation of the trend for each day, also during the daily controlled period (Fig. 15). In general, there was a slight overestimation of the results, with the only exception being the daytime of the thermal buffer (Day 4 in Fig. 14 - a). The local peak in the experimental data profile of the temperature values around 09:00 (see Fig. 14 - b) was likely due to direct irradiation of the temperature sensor, whose solar shield was possibly not perfect for ensuring all-day-long protection from the influence of the solar irradiance. At this time of the day, the shading device was off, and it was turned on at 10 a.m. The smaller peak in the simulation is likely to be a more realistic value that would have been recorded if the measuring device was not hit by solar irradiance impinging on the measurement point.

4.4. Prediction of surface heat flux (exchanged at the indoor-facing interface of the inner skin)

The readings from the surface heat flux meter included the longwave radiative and convective exchange between the indoor-facing surface of the inner glazing and the other surfaces and air of the room. The heat flux is probably the most complicated physical quantity to measure among those used in this validation process due to how the measurement is carried out and how the presence of the sensor modifies the physical phenomena locally. Even with all the precautions taken during the measurements, inaccuracy in the measurement is unavoidable due to the technology adopted. Inaccuracies are usually further amplified when the sensor is under solar irradiation. The sensors applied on the glazing surface increase the local absorptance of the glass in a way that cannot be represented in the simulation. Moreover, simplifying by averaging all the surface temperatures in one value may lead to errors connected to
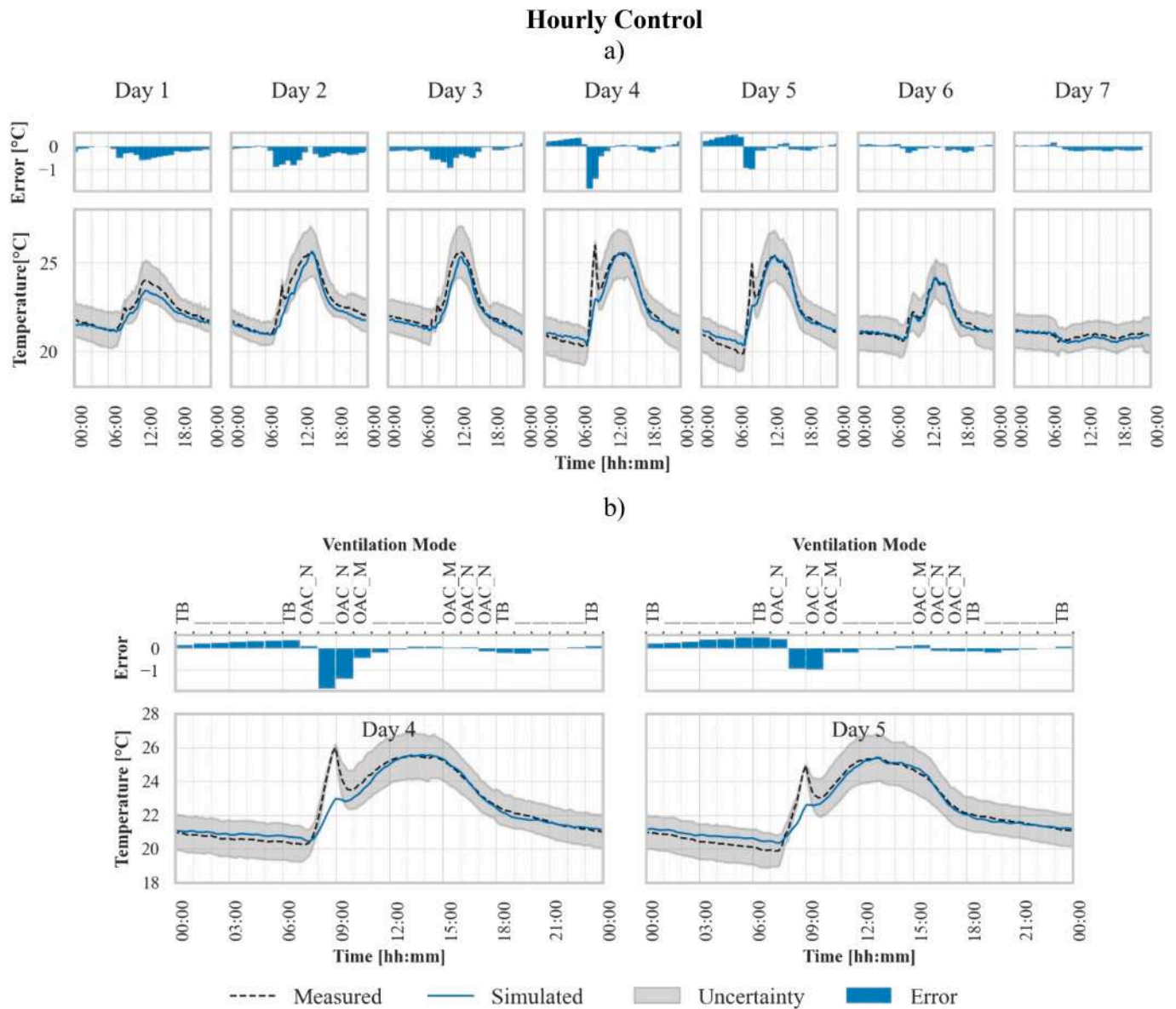
Hourly Control

a)

b)

Fig. 14. a) Time profile of the surface temperature for the hourly controlled days; b) detailed view of Day 4 and 5. The error is expressed in [°C]. The uncertainty band shows the two experimental values measured by the sensors on the surface.

the radiative exchange between surfaces. Considering the very good prediction of the inner glazing temperature and that the general trend of the heat flux was followed (with the maximum difference being ±10 W/m²), it seems that the model can reasonably predict the values of the surface heat flux (Figs. 16 and 17). The differences in magnitude between the heat flux under different configurations were well visible, and the peaks were aligned with the measured data.

5. Conclusion

The simulation work presented in this paper underlined the complexity of modelling a highly adaptive façade element, such as a

fully flexible DSF concept, using a BES tool. The need to adopt BES tools in predicting the short-term dynamic of a DSF is linked to the necessity of having an integrated environment to replicate the interactions between airflow in the façade, the HVAC system, and the building energy management system. The challenges are not only connected to the accuracy with which such tools can predict the performance of the DSF but also to the limitations that these tools present when it comes to adapting an existing element.

In this work we have: *i) demonstrated how to modify an existing routing* (*Double Glass Facade"*) available in a BES tool (IDA ice) to tackle that multi-path ventilation strategies in a DSF, enabling a flexible model to represent dynamic DSF systems that can switch between different
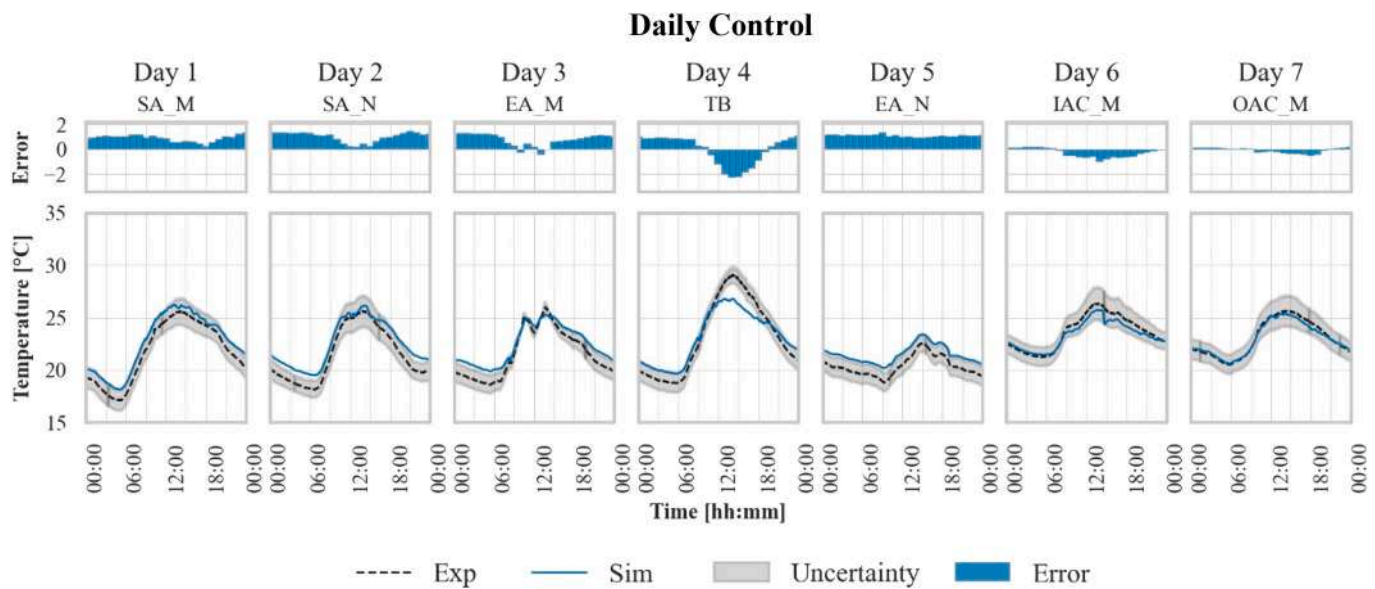
Fig. 15. Time profile of the surface temperature for the daily controlled days. The error is expressed in [°C]. The uncertainty band shows the two experimental values measured by the sensors on the surface.

ventilation modes (five flow paths – mechanically or naturally driven – and by-pass of the cavity) and driving force (natural and mechanical ventilation; *ii) compared the simulation results with experimental data from a dedicated measurement campaign* that covered a large range of operational modes, to assess and quantify the performance of the upgrade routine; *iii) verified that the model can replicate trends and dynamic profiles* of four main thermophysical quantities with mean bias errors lower than 1.5 °C and 4 W/m^2, for air and surface temperature values and for transmitted long-wave or short-wave heat flux values, respectively; *iv) quantified the simulation error for long-term* (e.g. 7 days) *energy simulations* that compute the thermal load on the room behind the façade, and this is, depending on the exact configuration and tested period, within the range of 5%–15%, which is considered suitable for energy simulations of buildings.

The enhanced model accurately depicts and approximates the switch from one configuration to the other. In terms of predictions, the airgap temperature is slightly overpredicted but much in line with the value measured in the higher portion of the cavity and is, therefore, more similar to what will be used from the outlets of the façade (i.e., a good approximation of the temperature used to climatise the indoor space). The surface temperature is in line with the mean measured value, which assures a good approximation for local discomfort analysis. The transmitted solar radiation is relatively well predicted, too, particularly if the position of the blinds is changed by a significant number of degrees. The heat flux estimation adequately depicts the daily profile of the incoming and exiting flux from the inner glazing, leading to a reasonable assessment of the overall energy calculation.

The limitations of the model we have developed in this study regarding simulation reliability are primarily linked to the limitations of the in-built DSF model of IDA ICE and not the alterations to match the functional features of the flexible DSF concept. By using an existing component within a BES tool, there is no possibility to intervene on the numerical assumptions of the component – unless further changes at the

level of the source code are implemented. For example, there is only one air gap node, so the temperature stratification inside of the cavity is not represented. Even if the openings are modelled with controllable elements, choosing the right values to use in order to model hinged openings is not straightforward; the definition of the leakage values for these openings when closed is of similar complexity.

Despite these limitations, the model presented in this work appeared to be a good trade-off for modelling a dynamic envelope like a DSF in terms of accuracy and model complexity. The enhanced model enables a vast range of variability in the façade, responding to the need for a flexible model that allows switching flow paths, controlling the degrees of openings and intertwining the room's active systems. In closing this article, in an effort to make our research freely accessible and to allow easy replication of our results, we make available, in an open-access repository, both the flexible DSF model developed in this research (Fig. 4) and the experimental dataset employed to validate the model. These can be found at and referenced using the following links: http://doi.org/10.5281/zenodo.7090264 [23] and http://doi.org/10.5281/zenodo.7090274 [48], for the model and the experimental dataset, respectively.

CRediT authorship contribution statement

Elena Catto Lucchino: Writing – original draft, Visualization, Validation, Software, Methodology, Investigation, Formal analysis, Data curation, Conceptualization. **Giovanni Gennaro:** Validation, Methodology, Investigation, Data curation, Writing – review & editing. **Fabio Favoino:** Writing – review & editing, Project administration, Methodology, Resources. **Francesco Goia:** Writing – review & editing, Supervision, Resources, Project administration, Methodology, Conceptualization, Formal analysis, Funding acquisition.
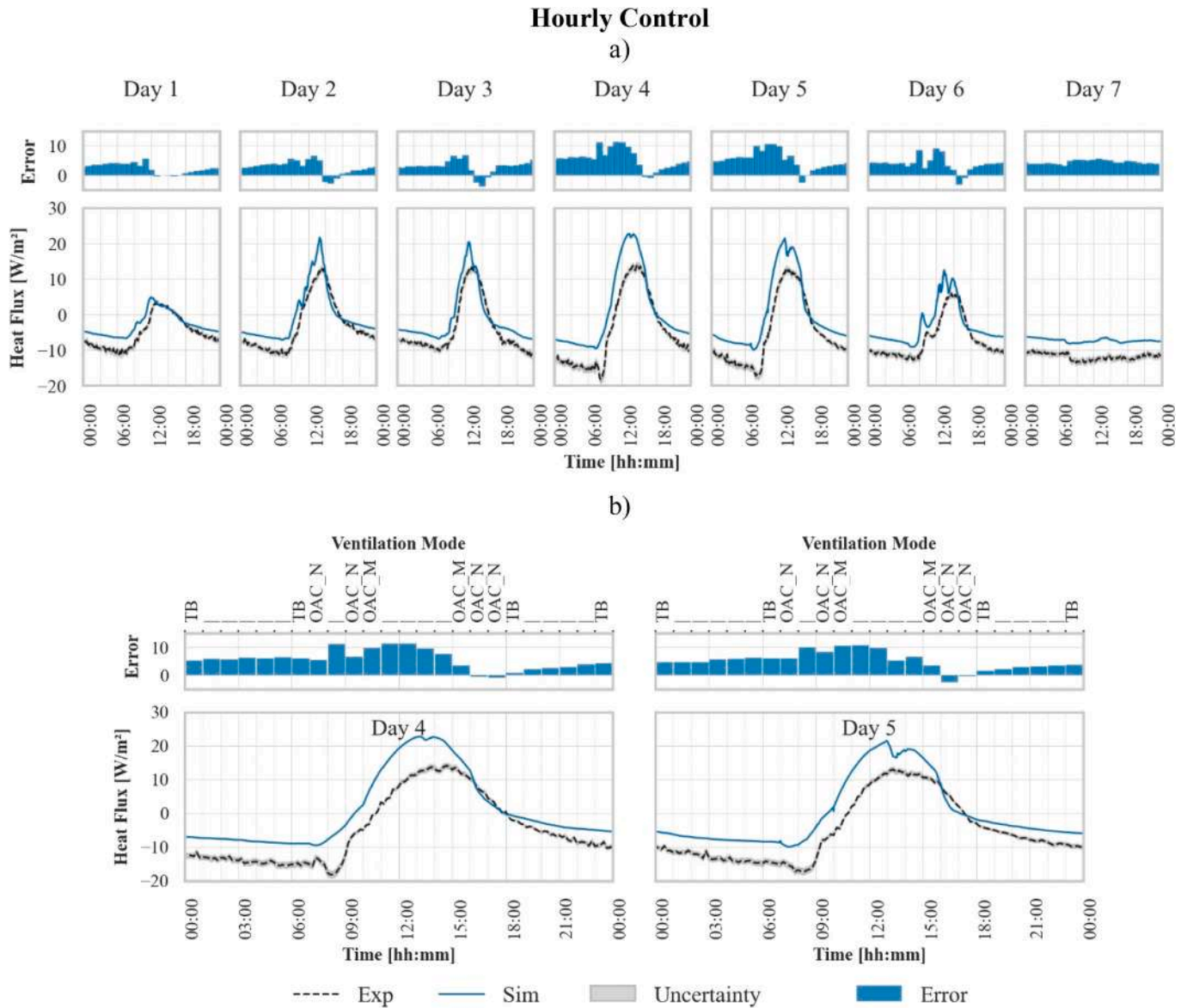
Hourly Control

a)

b)

Fig. 16. a) Time profile of the transmitted heat flux for the hourly controlled days; b) detailed view of Day 4 and 5. The error is expressed in [W/m²]. The uncertainty band shows the two experimental values measured by the heat flux meters.
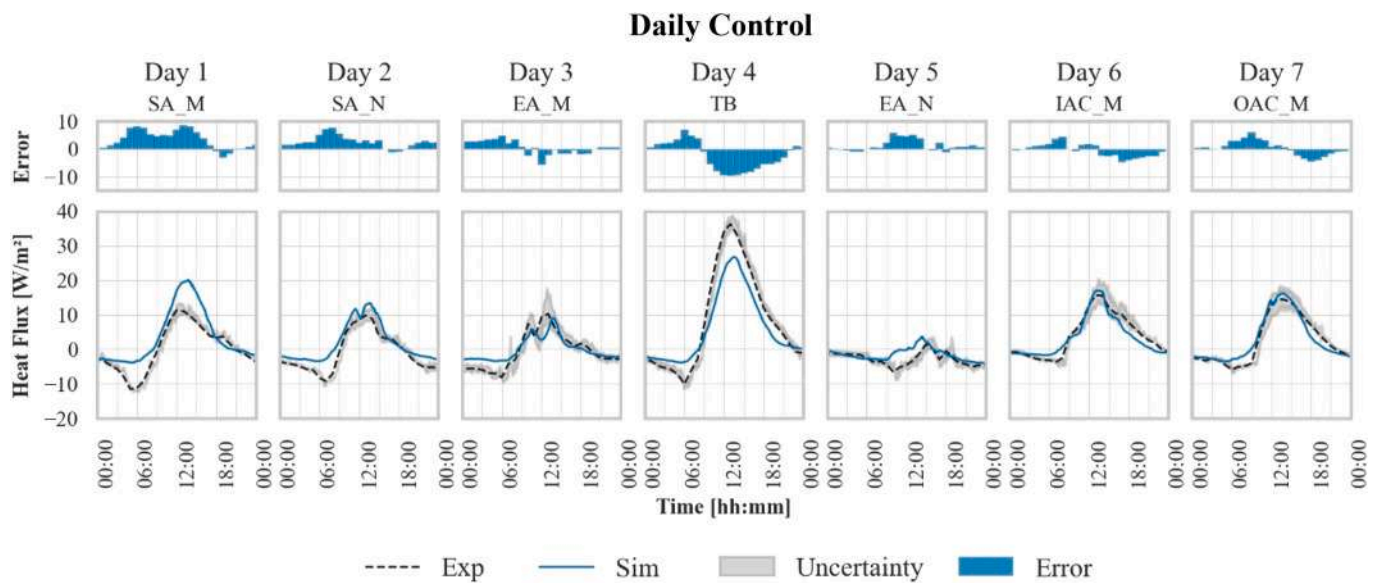
Daily Control

Fig. 17. Time profile of the transmitted heat flux for the daily controlled days. The error is expressed in [W/m^2]. The uncertainty band shows the two experimental values measured by the sensors on the surface.

Declaration of competing interest

The authors declare that they have no known competing financial interests or personal relationships that could have appeared to influence the work reported in this paper.

Data availability

The numerical model in IDA ICE and the experimental data for model validation are made available in an online repository as described in the article

Acknowledgement

References

[1] V. Huckemann, E. Kuchen, M. Leão, É.F.T.B. Leão, Empirical thermal comfort evaluation of single and double skin façades, Build. Environ. 45 (2010) 976–982, https://doi.org/10.1016/j.buildenv.2009.10.006.

[2] F. Pomponi, P.A.E. Piroozfar, R. Southall, P. Ashton, E.R.P. Farr, Energy performance of Double-Skin Façades in temperate climates: a systematic review and meta-analysis, Renew. Sustain. Energy Rev. 54 (2016) 1525–1536, https://doi.org/10.1016/j.rser.2015.10.075.

[3] M. Haase, F. Marques da Silva, A. Amato, Simulation of ventilated facades in hot and humid climates, Energy Build. 41 (2009) 361–373, https://doi.org/10.1016/j.enbuild.2008.11.008.

[4] A.S. Anđelković, I. Mujan, S. Dakić, Experimental validation of a EnergyPlus model: application of a multi-storey naturally ventilated double skin façade, Energy Build. 118 (2016) 27–36, https://doi.org/10.1016/j.enbuild.2016.02.045.

[5] U. Eicker, V. Fux, U. Bauer, L. Mei, D. Infield, Facades and summer performance of buildings, Energy Build. 40 (2008) 600–611, https://doi.org/10.1016/j.enbuild.2007.04.018.

[6] I. Khalifa, L.G. Ernez, E. Znouda, C. Bouden, Coupling TRNSYS 17 and CONTAM: simulation of a naturally ventilated double-skin facade, Adv. Build. Energy Res. 9 (2015) 293–304, https://doi.org/10.1080/17512549.2015.1050694.

[7] N.M. Mateus, A. Pinto, G.C. Da Graça, Validation of EnergyPlus thermal simulation of a double skin naturally and mechanically ventilated test cell, Energy Build. 75 (2014) 511–522, https://doi.org/10.1016/j.enbuild.2014.02.043.

[8] F. Pomponi, S. Barbosa, P.A.E. Piroozfar, On the intrinsic flexibility of the double skin façade: a comparative thermal comfort investigation in tropical and temperate climates, Energy Proc. 111 (2017) 530–539, https://doi.org/10.1016/j.egypro.2017.03.215.

[9] J.-S. Yu, J.-H. Kim, S.-M. Kim, J.-T. Kim, Thermal and energy performance of a building with PV-Applied double-skin façade, Proc. Inst. Civ. Eng. Eng. Sustain. 170 (2017), https://doi.org/10.1680/jensu.16.00017.

[10] R. Høseggen, B.J. Wachenfeldt, S.O. Hanssen, R. Hoseggen, B.J. Wachenfeldt, S. O. Hanssen, Building simulation as an assisting tool in decision making. Case study: with or without a double-skin facade? Energy Build. 40 (2008) 821–827, https://doi.org/10.1016/j.enbuild.2007.05.015.

[11] H. Elarga, A. Zarrella, M. De Carli, Dynamic energy evaluation and glazing layers optimization of façade building with innovative integration of PV modules, Energy Build. 111 (2016) 468–478, https://doi.org/10.1016/j.enbuild.2015.11.060.

[12] V. Leal, E. Erell, E. Maldonado, Y. Etzion, Modelling the SOLVENT ventilated window for whole building simulation, Build. Serv. Eng. Technol. 25 (2004) 183–195, https://doi.org/10.1191/0143624404bt103oa.

[13] A. Gelesz, A. Reith, Climate-based Performance Evaluation of Double Skin Facades by Building Energy Modelling in Central Europe, Energy Procedia, 2015, pp. 555–560, https://doi.org/10.1016/j.egypro.2015.11.735.

[14] N. Papadaki, S. Papantoniou, D. Kolokotsa, A parametric study of the energy performance of double-skin façades in climatic conditions of Crete, Greece, Int. J. Low Carbon Technol. 9 (2013) 296–304, https://doi.org/10.1093/ijlct/cts078.

[15] W. Choi, J. Joe, Y. Kwak, J.H. Huh, Operation and control strategies for multi-storey double skin facades during the heating season, Energy Build. 49 (2012) 454–465, https://doi.org/10.1016/j.enbuild.2012.02.047.

[16] C.S. Park, G. Augenbroe, Local vs. integrated control strategies for double-skin systems, Autom. ConStruct. 30 (2013) 50–56, https://doi.org/10.1016/j.autcon.2012.11.030.

[17] C.S. Park, G. Augenbroe, T. Messadi, M. Thitisawat, N. Sadegh, Calibration of a lumped simulation model for double-skin façade systems, Energy Build. 36 (2004) 1117–1130, https://doi.org/10.1016/j.enbuild.2004.04.003.

[18] C.S. Park, G. Augenbroe, N. Sadegh, M. Thitisawat, T. Messadi, Real-time optimization of a double-skin façade based on lumped modeling and occupant preference, Build. Environ. 39 (2004) 939–948, https://doi.org/10.1016/j.buildenv.2004.01.018.

[19] S.H. Yoon, C.S. Park, G. Augenbroe, On-line parameter estimation and optimal control strategy of a double-skin system, Build. Environ. 46 (2011) 1141–1150, https://doi.org/10.1016/j.buildenv.2010.12.001.

[20] D. Kim, C.-S. Park, A Heterogeneous System Simulation of a Double-Skin Façade, 12th Int. IBPSA Conf, Sydney, 2011, pp. 14–16, in: http://ibpsa.org/proceedings/BS2011/P_1281.pdf.

[21] E. Catto Lucchino, A. Gelesz, K. Skeie, G. Gennaro, A. Reith, V. Serra, F. Goia, Modelling double skin façades (DSFs) in whole-building energy simulation tools: validation and inter-software comparison of a mechanically ventilated single-story DSF, Build. Environ. 199 (2021), https://doi.org/10.1016/j.buildenv.2021.107906.

[22] E. Catto Lucchino, F. Goia, G. Lobaccaro, G. Chaudhary, Modelling of double skin facades in whole-building energy simulation tools: a review of current practices and possibilities for future developments, Build. Simulat. 12 (2019) 3–27, https://doi.org/10.1007/s12273-019-0511-y.

[23] E. Catto Lucchino, G. Gennaro, F. Favoino, F. Goia, Model for a Single-Storey Flexible Double-Skin Façade System in IDA ICE, 2022, https://doi.org/10.5281/zenodo.7090264.

[24] S. Kropf, G. Zweifel, Validation of the building simulation program IDA-ICE according to CEN 13791 "thermal performance of buildings - calculation of internal temperatures of a room in summer without mechanical cooling - general criteria and validation procedures, Adv. HVAC Nat. Gas Technol. 24 (2001). http://www.equaonline.com/iceuser/validation/ICE_vs_prEN 13791.pdf.

[25] EQUA, Validation of IDA indoor climate and energy 4 . 0 with respect to CEN standards EN 15255-2007 and EN 15265-2007, Http://Www.Equaonline.Com/Iceuser/Validation/. (2010) 19, http://www.equaonline.com/iceuser/validation/CEN_VALIDATION_EN_15255_AND_15265.pdf.

[26] A.B. EQUA Simulation, Validation of IDA Indoor Climate and Energy 4.0 Build 4 with Respect to ANSI/ASHRAE Standard 140-2004, ASHRAE Stand., 2010, p. 44.

[27] M. Vuolle, A. Bring, P. Sahlin, An NMF based model library for building thermal simulation, in: Proc. 6, Th IBPSA Conf., Kyoto, Japan, 1999, pp. 1–8.

[28] P. Sahlin, L. Eriksson, P. Grozman, H. Johnsson, A. Shapovalov, M. Vuolle, Whole-building simulation with symbolic DAE equations and general purpose solvers, Build. Environ. 39 (2004) 949–958, https://doi.org/10.1016/j.buildenv.2004.01.019.

[29] E. Taveres-Cachat, F. Favoino, R. Loonen, F. Goia, Ten questions concerning co-simulation for performance prediction of advanced building envelopes, Build. Environ. 191 (2021), https://doi.org/10.1016/j.buildenv.2020.107570.

[30] R.C.G.M. Loonen, F. Favoino, J.L.M. Hensen, M. Overend, Review of current status, requirements and opportunities for building performance simulation of adaptive facades, J. Build. Perform. Simul. 10 (2017) 205–223, https://doi.org/10.1080/19401493.2016.1152303.

[31] Y. Wang, Y. Chen, J. Zhou, Dynamic modeling of the ventilated double skin façade in hot summer and cold winter zone in China, Build, Environ. Times 106 (2016) 365–377, https://doi.org/10.1016/j.buildenv.2016.07.012.

[32] Y. Li, J. Darkwa, G. Kokogiannakis, Heat transfer analysis of an integrated double skin façade and phase change material blind system, Build. Environ. 125 (2017) 111–121, https://doi.org/10.1016/j.buildenv.2017.08.034.

[33] A. Dama, D. Angeli, O. Kalianova Larsen, Naturally ventilated double-skin façade in modeling and experiments, Energy Build. 144 (2017) 17–29, https://doi.org/10.1016/j.enbuild.2017.03.038.

[34] R.C.G.M. Loonen, F. Favoino, J.L.M. Hensen, M. Overend, Review of current status , requirements and opportunities for building performance simulation of adaptive facades, J. Build. Perform. Simul. (2016) 1–19, https://doi.org/10.1080/19401493.2016.1152303.

[35] A. Gelesz, E. Catto Lucchino, F. Goia, V. Serra, A. Reith, Characteristics that matter in a climate façade: a sensitivity analysis with building energy simulation tools, Energy Build. 229 (2020), https://doi.org/10.1016/j.enbuild.2020.110467.

[36] E. Catto Lucchino, F. Goia, G. Lobaccaro, G. Chaudhary, Modelling of double skin facades in whole-building energy simulation tools: a review of current practices and possibilities for future developments, Build. Simulat. 12 (2019), https://doi.org/10.1007/s12273-019-0511-y.

[37] ISO 15099, Thermal Performance of Windows, Doors and Shading Devices: Detailed Calculations, 2003.

[38] ISO 52022-3:20, ISO 52022-3, Energy Performance of Buildings - Thermal, Solar and Daylight Properties of Building Components and Elements - Part 3: Detailed Calculation Method of the Solar and Daylight Characteristics for Solar Protection Devices Combined with Glazing, 2017.

[39] A.B. EQUA Simulation, User Manual IDA Indoor Climate and Energy 4.8 (2018).

[40] A. Gelesz, E. Catto Lucchino, F. Goia, A. Reith, V. Serra, Reliability and sensitivity of building performance simulation tools in simulating mechanically ventilated double skin facades, in: V. Corrado, A. Gasparella (Eds.), Proc. Build. Simul. 2019 16th Conf, IBPSA, Rome, 2019.

[41] G. Gennaro, E. Catto Lucchino, F. Goia, F. Favoino, Modelling double skin façades (DSFs) in whole-building energy simulation tools: validation and inter-software comparison of naturally ventilated single-story DSFs, Submitt. to Build. Environ. (2022) (Submission Nr. BAE-D-22-03720).

[42] F. Goia, V. Serra, Analysis of a non-calorimetric method for assessment of in-situ thermal transmittance and solar factor of glazed systems, Sol. Energy 166 (2018) 458–471, https://doi.org/10.1016/j.solener.2018.03.058.

[43] J.M. Bright, N.A. Engerer, Engerer2: global re-parameterisation, update, and validation of an irradiance separation model at different temporal resolutions, J. Renew. Sustain. Energy 11 (2019), https://doi.org/10.1063/1.5097014.

[44] J.-N. Hersbach H, B. Bell, P. Berrisford, G. Biavati, A. Horányi, J. Muñoz Sabater, J. Nicolas, C. Peubey, R. Radu, I. Rozum, D. Schepers, A. Simmons, C. Soci, D. Dee, Thépaut, ERA5 hourly data on single levels from 1979 to present, in: Copernicus Climate Change Service (C3S) Climate Data Store (CDS), 2018, https://doi.org/10.24381/cds.adbb2d47. (Accessed 26 April 2021). Accessed on.

[45] TRNFLOW, 56, in: A Module of an Air Flow Network for Coupled Simulation with TYPE 56 (Multi-zone Building of TRNSYS), 2009, pp. 1–58.

[46] EQUA Simulation AB, IDA –Indoor Climate and Energy Ver 3.0 NMF-Model Documentation, ((n.d.)).

[47] ASHRAE, ASHRAE Guideline 14 - Measurement of Energy, Demand, and Water Savings, 2014.

[48] E. Catto Lucchino, G. Gennaro, F. Favoino, F. Goia, Experimental Data for Validation of a Single-Storey Flexible Double-Skin Façade System Model, 2022, https://doi.org/10.5281/zenodo.7090274.